ANCHORED LOG DECKS

By

Evangeline Rivera Murison

A Thesis submitted to the Faculty of Graduate Studies
of the University of Manitoba
in partial fulfillment of the requirements for the degree of

Master of Science

Department of Civil Engineering
University of Manitoba
Winnipeg, Manitoba, Canada

TABLE OF CONTENTS

ABSTRACT

To improve the performance of the conventional nail laminated bridge deck, three generations of innovative decks have been developed during the last three decades: (a) the stress laminated wood deck, (b) the stressed log bridge, and (c) the grout laminated wood deck. The grout laminated wood deck, the most recent wood deck, consists of trimmed logs interconnected with internal grout cylinders, in compression or tension. Previous research has shown that the grout cylinders have superior load distribution characteristics, but the cost of trimming the treated logs was found to be relatively high. Recently, research has been conducted to develop the next generation of the bridge wood decks, called the anchored log decks. The anchored log deck, meant for use as decking of steel girder bridges, consists of untrimmed discarded utility timber poles which have been treated with preservatives. The logs are held together by means of unstressed transverse proprietary Cintec anchors. The anchors consist of stainless steel rods encased in grout cylinders. Panels, each comprising of 5 to 6 logs, are preassembled to fit on a flatbed trailer for shipping. The smooth wearing surface over the log deck is provided by longitudinal sawn timber planks, with high-density foam filling the gap between the logs and the planks. The panels are inter-connected through inclined anchors passing through adjacent logs. At the University of Manitoba, an anchored log deck with five preassembled panels was constructed and tested to failure at several locations under both static and fatigue loads. The test results have shown that anchored log decks have the potential of being economical preassembled decks for steel girder bridges.

ACKNOWLEDGEMENTS

I would like to express my appreciation and gratitude to my advisor, Dr. Aftab Mufti, for his advice, supervision, encouragement and financial support throughout my research. I would also like to thank my co-advisor, Dr. Dagmar Svecova, for her insight and guidance. The work presented in this thesis would not have been possible without their advice and support.

I would also like to thank the technical staff at the W.R. McQuade Structures Lab including Mr. Chad Klowak, Mr. Grant Whiteside and Mr. Brendan Pachal. Their technical assistance in this research work is greatly appreciated. Furthermore, I would like to thank Mr. Geoffrey Cao, Dr. Liting Han and Mr. Tim Reeve for their assistance in the lab.

I would like to express my gratitude to Dr Baidar Bakht whose advice and guidance in this work has been invaluable.

I would like to acknowledge the financial contribution of the National Science and Engineering Research Council of Canada. I am also thankful to Cintec Canada for the contribution of their anchoring technology for this research work.

Finally, I would like to thank my family and friends for their support and understanding. I would like to especially thank my husband Scott for his patience, encouragement and love.

LIST OF TABLES

LIST OF FIGURES

LIST OF SYMBOLS

DF	=	distribution factor
E	=	modulus of elasticity
EI	=	bending stiffness
G	=	shear modulus
I	=	moment of inertia
J	=	torsional moment of inertia
δ	=	deflection

LIST OF ABBREVIATIONS

CHBDC	=	Canadian Highway Bridge Design Code
FRP	=	Fibre Reinforced Polymer
GFRP	=	Glass Fibre Reinforced Polymer
GLWD	=	Grout Laminated Wood Deck
LVDT	=	Linear Variable Displacement Transducer
SLB	=	Stressed Log Bridge
SLWD	=	Stressed Laminated Wood Deck

1. Introduction

1.1 Background

Beginning in the late 19th century, concrete and steel slowly replaced the use of timber for the construction of bridges. However, timber bridges are still considered for use in short and medium span structures.

The winter road network in Manitoba is an integral part of the transportation system in the northern and remote communities. During the winter season, from mid-January to mid-March every year, ice roads are cleared to facilitate transportation of goods and freight. The roads provide a means to travel between remote communities and the rest of the province. The network spans over 2000 kilometers long and provides access to approximately 30 communities with a total population of over 29,000 people. (Kuryk 2003).

As part of the winter road network, temporary bridges are constructed to cross small streams and creeks. The main issues with winter road bridge structures are the increased costs due to remoteness, winter construction and limited access. The bridges currently being used by the Province of Manitoba are "Mechano" type bridges (Kuryk 2003). These bridges are difficult to transport due to their weight, are labour intensive to install and cannot be removed easily at the end of the winter season. Thus, there is a need for simple, light and reliable alternatives to traditional winter bridges.

In North America, preservative-treated timber poles are commonly used as utility poles and every year, a large number are removed from service for a variety of reasons, and are usually discarded. Many of these discarded poles have their structural integrity intact and could be used for structural applications (Limaye 1999). The use of timber poles for winter road bridge structures is ideal for several reasons including: (a) the handling of material does not require highly skilled labour, (b) the preservative treatment ensures high durability, and (c) the use of difficult-to-discard treated poles is environment-friendly, and (d) the bridge decks are cost-effective.

Earlier timber bridges were constructed using nail and stress lamination techniques. Although nail laminated timber decks were economical and easy to construct, they were susceptible to a reduction in load distribution characteristics due to the loosening of the nail connections under repeated loading. A solution to this problem was the development of stress laminated wood decks. In this technique, the timber laminates are compressed laterally by post-tensioning through steel tendons. While this method provided a solution to rehabilitate nail laminated wood decks, it required periodic re-stressing of the tendons to maintain the required prestress levels.

This led to the development of the grout laminated wood deck and the use of grout cylinders to facilitate transverse load distribution. The grout cylinders are located transversely through the deck and consist of stressed steel or glass fibre reinforced polymer (GFRP) bars surrounded by grout. This results in grout cylinders which are in either compression or tension, depending on the procedure in which the reinforcing bars

are stressed. Research has found that the grout cylinders, in either tension or compression, can successfully transfer the load by acting as shear keys between the logs.

1.2 Objective and Scope

The objective of this study is to investigate the performance of the next generation of wood bridge decks, called the anchored log decks. By removing the requirement for a prestressing system, this will simplify the construction process and lower the overall cost of the bridge deck.

The scope of work conducted in this study has the following components.

- Construct three log assemblies to determine the performance of unstressed grout cores.
- Construct a model of an anchored log deck with unstressed grout cores.
- Test the log deck under monotonically increasing (static) and fatigue loads.
- Evaluate the performance of the deck design through analysis of the sensor data from both the static and fatigue tests.
- Compare the static test results from the bridge deck with the results from SECAN, a program based on the semi-continuum method of analysis.
- Develop recommendations for future work.

1.3 Thesis Organization

This thesis is comprised of six chapters. A brief literature review of traditional wood bridge decks is discussed in Chapter 2. The construction of the specimens and the experimental test setup are described in Chapter 3. In Chapter 4, instrumentation schemes

and experimental results are presented and an analysis of experimental data is discussed in Chapter 5. Finally, the conclusions and recommendations for future research are presented in Chapter 6. A list of references is provided at the end of this thesis.

2. Literature Review

2.1 Overview

Timber bridges were the earliest bridges constructed in human history. As timber was a readily available and abundant resource, it was considered a fundamental building material. The advantages of wood as a bridge material include its light weight, and high strength and durability. This section provides a description of wood bridge decks that have been developed and constructed in the last century.

2.2 Nail Laminated Wood Decks

For a period of 40 years between the 1920's to the 1960's, nail laminated wood decks were the most common types of timber deck constructed in North America (Ritter 1990); these decks were used as superstructures for short span bridges, or as decks on medium span girder bridges. The decks were constructed by placing dimensional lumber pieces (laminates) on their edges and attaching them successively to the adjacent lumber pieces through nails (Figure 2-1). The load transfer between adjacent lumber pieces is achieved through the nails.

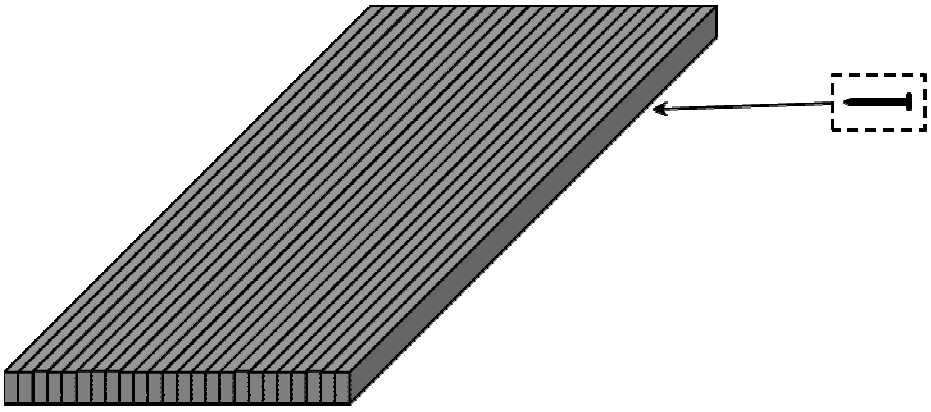

Figure 2-1. Nail laminated timber deck.

The advantage of nail laminated wood decks is their ease of construction which makes them an economical option as a bridge deck. However, these decks are susceptible to deterioration of their transverse load distribution characteristics due to the gradual loosening of the nail connections under repeated loads. As the deck experiences fatigue loading and changes in moisture, the nails can work themselves loose and as a result, the load is not fully distributed to adjacent sections. Over time, this results in an increase in deflections of the directly loaded laminates and the consequent cracking of the wearing course. The use of nail laminated decks decreased as other types of decks were developed.

2.3 Stress Laminated Wood Decks and Stressed Log Bridges

Stress laminated timber bridges were developed in Ontario and its first implementation on a bridge was in 1976 (Csagoly and Taylor 1980). In these decks, the laminates are compressed together laterally by stressed steel bars located either outside the deck (Figure 2-2), or inside (Figure 2-3). By compressing the laminates, the dependence on the nail connections is eliminated for load distribution. The stiffness of the deck increases considerably by the reduction of the rotation of the laminate ends at the butt joints, thus increasing its load capacity. The stress lamination technique can be used to rehabilitate nail laminated wood decks as well as for new construction.

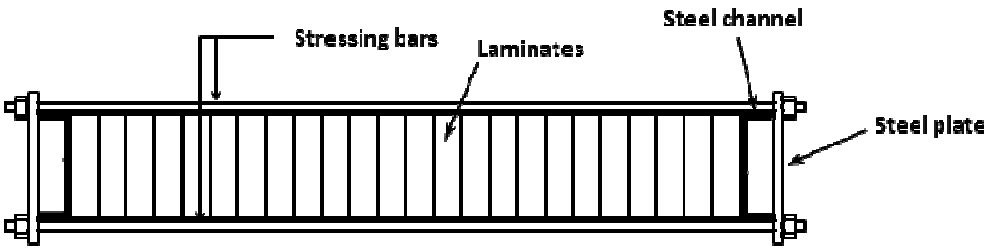

Figure 2-2. External stress lamination configuration.

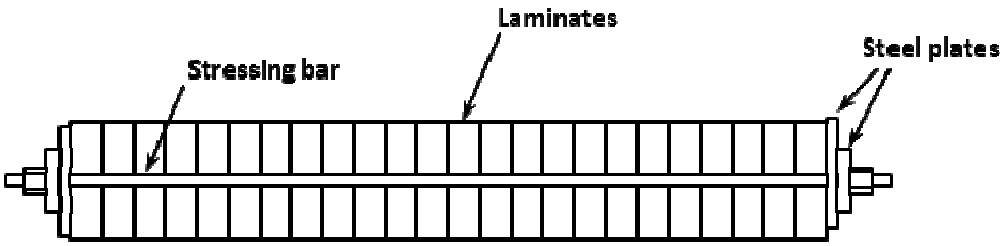

Figure 2-3. Internal stress lamination configuration.

The main disadvantage in stress lamination is the large prestress losses in the steel tendons. Creep and changes in moisture content in the timber largely contribute to the prestress loss in the steel bars. According to the Canadian Highway Bridge Design Code (CHBDC 2000), restressing of the bars is required at least two times within four weeks of the initial stressing during construction of the deck. Bakht et al. (1994) observed the behavior of five stress laminated wood decks over a 19 year period. From these field observations, it was found that the prestress losses were large enough to drop below the minimum level required by CHBDC (2000). However, periodic re-stressing can help maintain the prestress levels above the minimum required level.

As an extension of the stress laminated wood deck, research (Bakht et al. 1996) was conducted to develop the stressed log bridge. This bridge concept focused on the use of discarded utility timber poles and low modulus tendons to reduce prestress losses. The tendons evaluated in this research were made of Aramid and glass fibres. Decks were constructed with timber poles that were trimmed to have two parallel faces (Figure 2-4). From the research, it was concluded that, although the use of Aramid tendons did reduce the prestress losses, they are not a feasible option due to the high cost of the tendons and the anchors. A stressed log bridge was constructed in Northern Ontario which used glass fibre reinforced polymer (GFRP) tendons in 1996 (Bakht et al. 1997). During

construction of the bridge, there were issues with the anchors which secured the GFRP tendons. Unfortunately, this is the only stressed log bridge that has been constructed to date in the field.

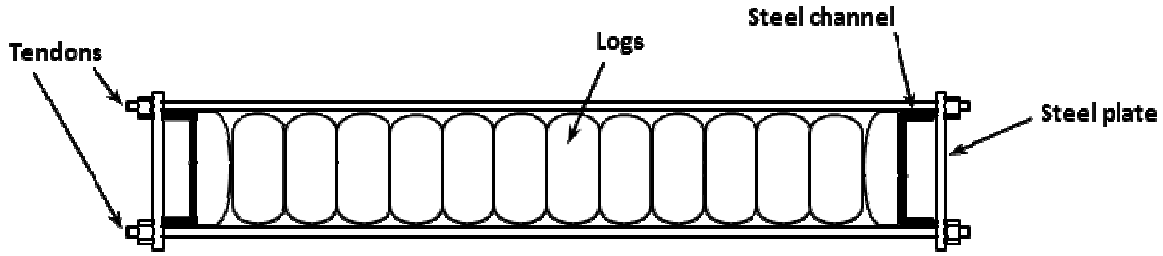

Figure 2-4. Stressed log deck.

2.4 Grout Laminated Wood Decks

The third generation of the stress laminated wood deck was the grout laminated wood deck (Limaye 1999). This deck consisted of internal grout cylinders which held the wood laminates together and acted as shear keys. As shown in Figure 2-5, the grout laminated wood deck consists of reinforced grout cores with non-shrink grout surrounding steel or GFRP bars. In his research, Limaye constructed and tested two full-scale wood deck panels. The decks each measured approximately 4 m by 2 m and were constructed with new untreated timber logs. The logs were trimmed flat on 3 sides leaving the top side as the only rounded face. The first deck incorporated steel reinforcing bars and was internally prestressed such that the grout cores were under compression. The second deck utilized GFRP bars and the grout cores were subjected to tension as the deck was externally prestressed prior to grouting.

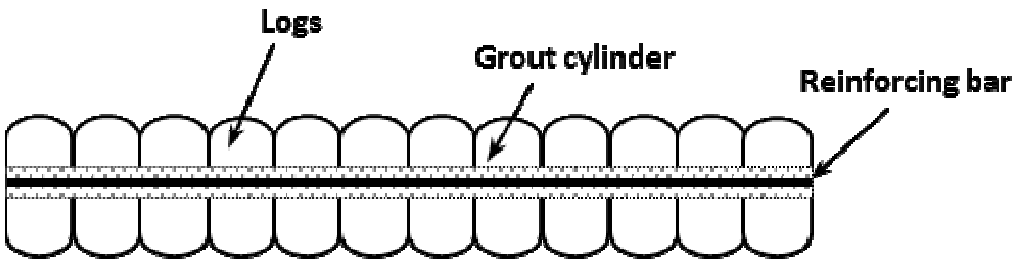

Figure 2-5. Grout laminated wood deck configuration.

Both decks were tested under a single static wheel load and the deflections of the logs were monitored during the testing. The decks were not tested to failure and the maximum applied load was 235 kN. Based on his test results, Limaye concluded that the grout cores were successful in transferring the load to adjacent logs. The grout cylinders which were in compression performed better than the cylinders in tension which developed cracks after the release of the external prestressing system.

In continuation of this research, destructive testing of the two decks was conducted at the University of Manitoba (Klowak 2001), 23 months after Limaye's tests. For each deck, a monotonically increasing load was applied until failure. This research confirmed the effectiveness of the load distribution characteristics of the grout cores. It was also noted that although the grout laminated decks did suffer from prestresss loss over time, these losses were smaller than the losses in stress laminated decks. The testing conducted on the grout laminated wood deck demonstrated the validity of the concept.

3. Experimental Program

3.1 Introduction

The experimental program was carried out at the McQuade Structures Laboratory at the University of Manitoba. The program involved the design, construction and testing of eight models of three log assemblies and one model of an anchored log bridge deck. All logs used in the test program were discarded utility poles, donated by Manitoba Hydro.

3.2 Material

One goal of the research program was to determine the feasibility of using discarded utility poles for the construction of deck panels. There are over one million hydro poles (Figure 3-1) in service in Manitoba. Every month, the number of poles removed from service can range from tens to hundreds. When the poles are removed from service, they are inspected and those that are still considered serviceable are returned to inventory for re-use. Those that are deemed unserviceable are disposed of from the pole yards and made available to the public. The material is often used for pole barns, wood piles, and fence posts; and may be re-sawn to lumber for outdoor use. For this work, the poles were obtained from Manitoba Hydro.

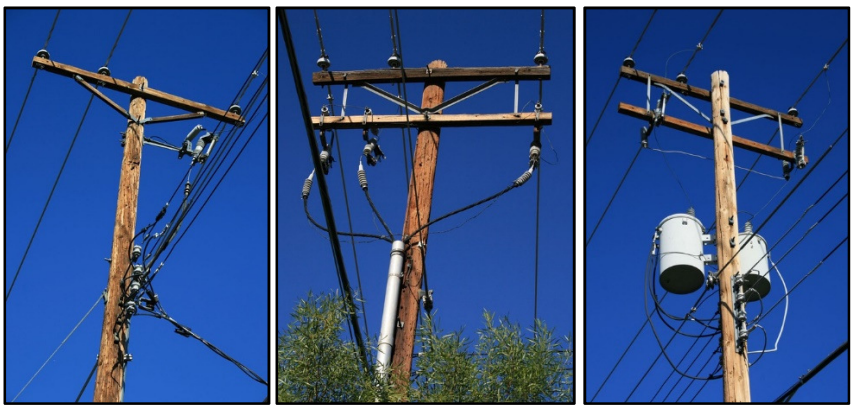

Figure 3-1. Hydro poles.

The species of most of the timber poles used by Manitoba Hydro are either cedar or pine. The cedars are almost exclusively Western Red Cedar with some being Yellow Cedar. As for the pine species, the current species is the Lodge Pole Pine; however, there are Jack Pine and Red Pine in the system as well.

There are currently two wood preservatives used for treating the poles. The first is Chromated Copper Arsenate (CCA) which is a water-based green-coloured preservative. The second is Pentachlorophenal (Penta) which is an oil-based brown-coloured preservative. The preservatives protect the wood against organisms such as termites and fungi. The timber logs used in the experimental program were a random mix of cedar and pines species treated with either the CCA or Penta preservative; some of the poles used in the experimental program are shown in Figure 3-2.

Figure 3-2. Timber logs for deck panels.

3.3 Grout Lamination

The concept of grout lamination was introduced by Dr Aftab Mufti and Dr Baidar Bakht in 1997 (Limaye 1999). It was developed to eliminate the effect of prestress loss in stress laminated wood decks.

Grout lamination consists of reinforced grout cores installed transversely along the deck at fixed intervals. The purpose of the grout cores is to provide a load transfer between the laminates by acting as shear keys.

The grout cores are installed in transverse holes drilled in the deck. Reinforcing bars, either steel or FRP, are installed in the holes and grout is injected (Figure 3-3). Previous research in grout lamination has involved decks constructed with the grout cylinders in compression or tension. This research will investigate the performance of unstressed grout cylinders.

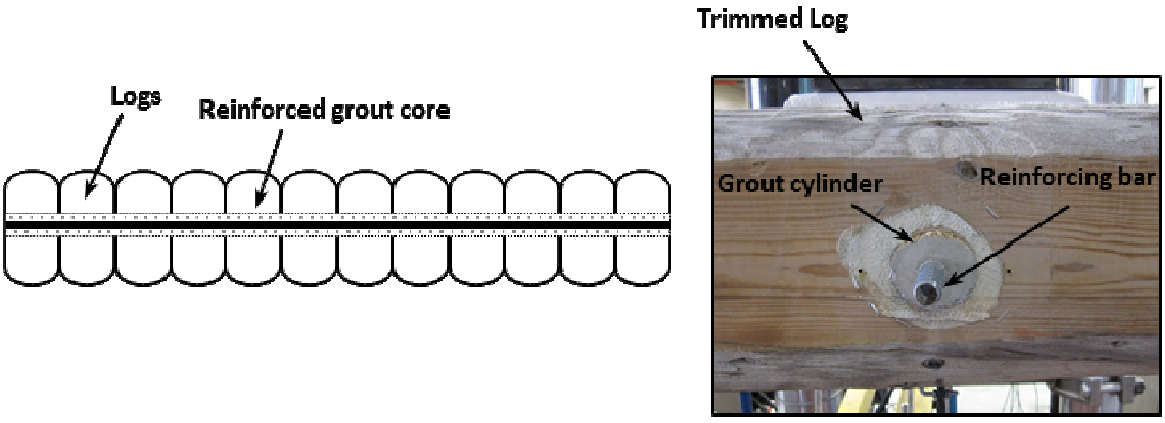

Figure 3-3. Grout lamination concept.

3.4 Three Log Assemblies

3.4.1 Design

The three log assemblies (panels) each consisted of three logs with a length of 2400 mm. Panels with round logs and planed logs were constructed for testing. The heights of the logs ranged from 195 to 290 mm. The planed logs were trimmed on two parallel faces to a width of 180 mm. Each log had a 50 mm hole drilled at mid-span and mid-height.

3.4.2 Preparatory Work

Prior to the assembly of each panel, the bending stiffness (ie. the product of elastic modulus (E) and moment of inertia (I)) was determined experimentally for each log. To accomplish this, each log was placed in the MTS testing machine and subjected to a concentrated load at mid-span. The log was supported by roller supports spaced 2100 mm apart (Figure 3-4).

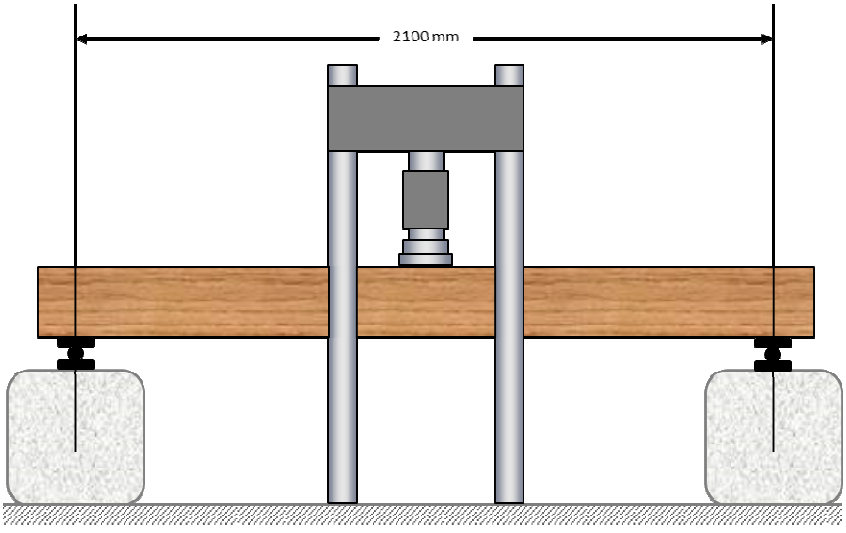

Figure 3-4. Test setup for stiffness tests.

Deflection was measured using a linear variable displacement transducer (LVDT) located at the mid-span. A monotonically increasing load was applied to a maximum load of

30 kN. Load and deflection data recorded from the test was then used to calculate the bending stiffness (EI) value for each log. The equation for the maximum deflection of a simply supported beam subjected to a point load at the mid-span is:

$$\delta = \frac{PL^3}{48EI} \quad [3\text{-}1]$$

Where, δ is the deflection at mid-span, P is the point load, L is the span of the beam, E is the modulus of elasticity of the log and I is the moment of inertia. Using P, L and δ from the test data, the EI value can be calculated for each log. Several logs were tested to failure to determine the maximum failure loads. The values of EI for the various logs are presented in Table 3-1.

Table 3-1. Values for EI for planed and round logs.

Planed Logs		**Round Logs**	
Log #	**EI (N/mm^2) x 10^{11}**	**Log #**	**EI (N/mm^2) x 10^{11}**
2	15.2	1	24.0
3	19.0	2	22.4
4	15.1	4	17.5
5	17.9	5	14.2
6	11.2	6	17.8
7	6.7	7	12.5
8	11.4	8	11.8
11	13.3	9	17.0
12	9.7	12	14.8

The panels were assembled based on the EI values obtained for each log. For each three log panel, the log with the smallest EI value was placed in the middle to ensure that the transverse shear in the shear key was high. The log combinations for the panels are summarized in Table 3-2.

Table 3-2. Log panel combinations.

Log Type	Set #	Outside Log #	Middle Log #	Outside Log #
Planed	1	5	6	3
	2	2	12	4
	3	8	7	11
Round	1	1	6	2
	2	4	12	9
	3	5	8	7

3.4.3 Construction

The logs were aligned using their central holes and held in place with timber boards at the ends (Figure 3-5). A total of six panels were constructed initially: three panels with planed logs and three with round logs. In preparation for grouting, a 15 mm steel reinforcing bar was installed in the center of each hole using wood plates on the outer logs (Figure 3-6). Small holes were drilled above the wood plates for injection of the grout. Grouting was conducted by a local contractor (Figure 3-7). The type of grout used was a non-shrink grout. Grout cubes were also prepared during the grouting process.

Figure 3-5. Timber boards holding planed logs in place.

Figure 3-6. Steel reinforcing bar and grout tube.

Figure 3-7. Grouting of log panels.

The spaces between the round logs were filled with putty to prevent the leakage of the grout. However, it was observed this was a time consuming and difficult process which did not always guarantee that there would be no leakage. As a result, two additional round log panels were constructed using patented anchoring technology from Cintec Ltd. This innovative technology consists of a 15.88 mm (5/8”) stainless steel threaded bar surrounded by a fabric material called the sock (Figure 3-8). Grout is then injected into the ‘sock’ which expands to fill the hole and contains the grout to prevent any leakage

(Figure 3-9). In this figure, it can also be seen that the sock expands in between the logs to effectively enclose the grout.

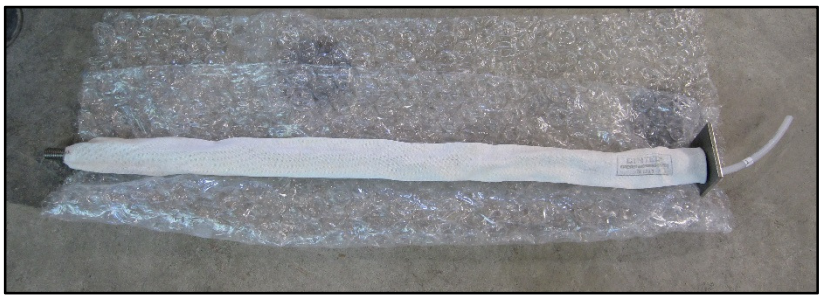

Figure 3-8. Cintec anchor with stainless steel bar and fabric sock.

Figure 3-9. Cintec anchor installed in log panel and expansion of sock with grout.

3.4.4 Test Setup

The three log panels were tested under monotonically increasing loading in the 5000 kN capacity MTS machine. The panels were mounted on steel roller supports spaced at 2100 mm. The panel was aligned such a way that the middle log was directly underneath the actuator. Since the grout holes were drilled at mid-height of each log and the logs varied in diameter, most logs were not in contact with the steel supports. To ensure direct contact of the logs with supports, grout was dry-packed underneath the logs (Figure 3-10). A steel loading plate with dimensions of 250 x 150 x 18 mm was placed at the mid-

span of the middle log (Figure 3-11). Plaster was placed in between the log and the plate to create a flat surface for the loading plate, which was used to load only the middle log. The purpose of these tests was to determine the amount of load passed on from the directly loaded log to the adjacent logs.

Figure 3-10. Grout placed underneath logs at supports in small-scale assemblies.

Figure 3-11. Static test setup and load plate at middle log.

3.4.5 Static Testing

A monotonically increasing load, referred to herein as the 'static' load, was applied at a rate of 2 mm per minute. During the loading process, deflections and magnitude of load were recorded continuously by the data acquisition system. The loading was increased until failure of the panel.

One panel with planed logs and two panels with round logs, each with a grout core at the mid-span, were initially tested under static loading. Upon analysis of the data, it was decided to add grout cores to the remaining panels at the quarter span locations to improve the load distribution (Figure 3-12). The panels were then tested to failure under static loading.

Figure 3-12. Additional grout cores at quarter span.

3.5 Model of Anchored Log Deck

3.5.1 Design

The model of the anchored log deck comprised of a total of five log panels each consisting of 5 or 6 logs. The logs were 4300 mm in length and the diameters of the logs ranged from 200 to 300 mm. The logs were not trimmed due to the high cost of this work. Four 50 mm diameter holes were drilled in each log at a spacing of 1080 mm longitudinally, beginning 530 mm from each end (Figure 3-13). The holes were drilled at a distance of 100 mm from the bottom face of the log.

Figure 3-13. Logs for the anchored log deck with holes drilled at four locations.

3.5.2 Preparatory Work

For the model of the anchored log deck, the logs were not tested to determine their individual modulus of elasticity and moment of inertia. It can be justified that if these logs were to be used in the field, they would be chosen randomly without prior knowledge of their sectional and material properties.

The log panels were constructed as if they would be used in the field. The dimensions of the panels were such that they would fit on a flatbed trailer for shipping. This resulted in assembling panels with 5 or 6 logs to create a panel width of approximately 1524 mm (5'). Similar to the three log assemblies, the logs were aligned according to the four drilled holes and held together with timber boards (Figure 3-14). Due to the taper of the logs, the logs were oriented by alternating the taper between adjacent logs (i.e., placed alternately tip to butt). The goal was to result in a somewhat 'square' panel. Cintec anchors consisting of 15.88 mm (5/8") stainless steel bars were installed and grouted in each of the cores. The operation of grouting the anchors is illustrated in the photographs presented in Figure 3-15.

Figure 3-14. Full-scale panels with end boards.

Figure 3-15. Grouting of Cintec anchors.

3.5.3 Construction

Two steel girders were placed at a center-to-center distance of 3500 mm. Each girder 425 mm wide, 925 mm deep, and 9000 mm long. The girders were placed on four concrete bearing blocks. The log panels were placed side by side on the girders. Although most of the logs were in contact with the girder, there were some logs that required shims underneath. Clip angles were used to attach the panel to the girder (Figure 3-16). The angles consisted of steel plates with notches to fit around the flange thickness and attached to the log with common nails. The steel plates were 102 x 305 x 9.5 mm (4" x 12" x 3/8") thick.

Figure 3-16. Placement of panels on girders and steel clip angle.

After the panels were placed on the girders, adjacent panels were connected to each other using 50 mm diameter, 305 mm long (1/2" x 12") lag screws drilled diagonally and staggered along with width of the deck. The external logs of two adjacent panels were connected by drilling a diagonal hole from one log to the other and inserting a lag screw through the hole (Figure 3-17). Timber wearing planks were installed on the surface of the deck using lag screws. The planks consisted of four rows of 64 x 286 mm (3" x 12" with actual dimensions of 2.5" x 11.25") rough sawn oak planks placed side by side on

either half of the deck. The planks were located 450 mm from the centerline of the bridge.

Figure 3-17. Installation of lag screws to connect panels.

After installation of the planks, it was observed there were large gaps between the planks and the top of some logs. The planks were only in contact with the tallest logs. Thus, expansive spray foam was used to fill the gaps and provide a support material underneath the planks (Figure 3-18). The high density Polyurethane Resin foam is typically used by contractors for slab-jacking, void-filling and stabilizing concrete slabs. The density of the foam depends on the confinement and the compressive strength ranges from 0.6 MPa in an unconfined state and up to 10 MPa in a confined state (Concrete Restoration Services).

Figure 3-18. Gaps under wearing planks and high density foam.

3.5.4 Test Setup

The loading system consisted of a steel loading frame that was connected to the structural floor. A hydraulic actuator with a steel spreader beam was used to apply load through two steel plates at a spacing of 1.8 m. Each plate measured 610 mm in length and 305 mm in width to simulate the foot-print of a wheel of a CL-W truck (CHBDC 2000). Neoprene pads were placed between wearing planks and steel plates. The steel plates were located as eccentric to the wearing planks as possible. The test setup is shown in Figure 3-19. The actuator was used to apply both static and fatigue loads to the deck.

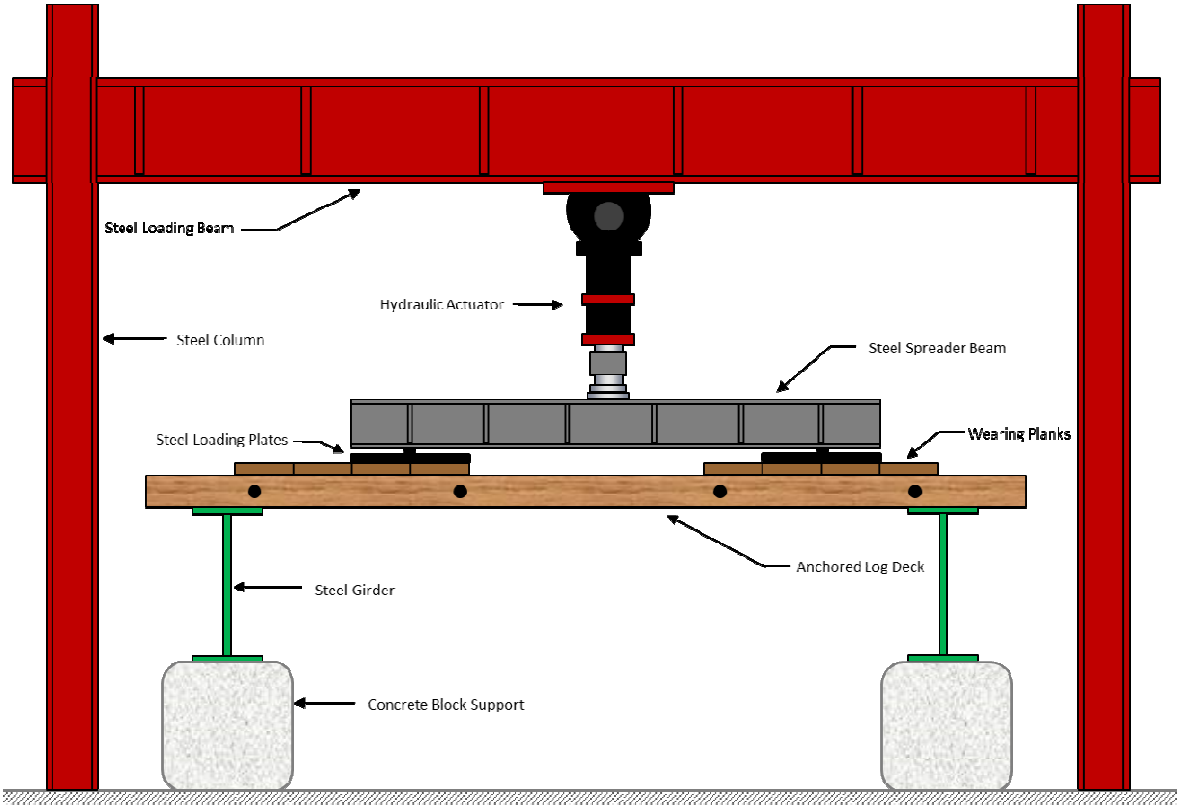

Figure 3-19. Test setup for anchored log bridge deck.

3.5.5 Test Locations

There were a total of two test locations on the anchored log deck: the first was located over the log (#1) at the end of the deck and the second was located over the log (#18) at the end of a panel near mid-span. The test locations are shown in Figure 3-20. Each location shows two steel loading plates which simulate the foot-print of a Cl-W truck.

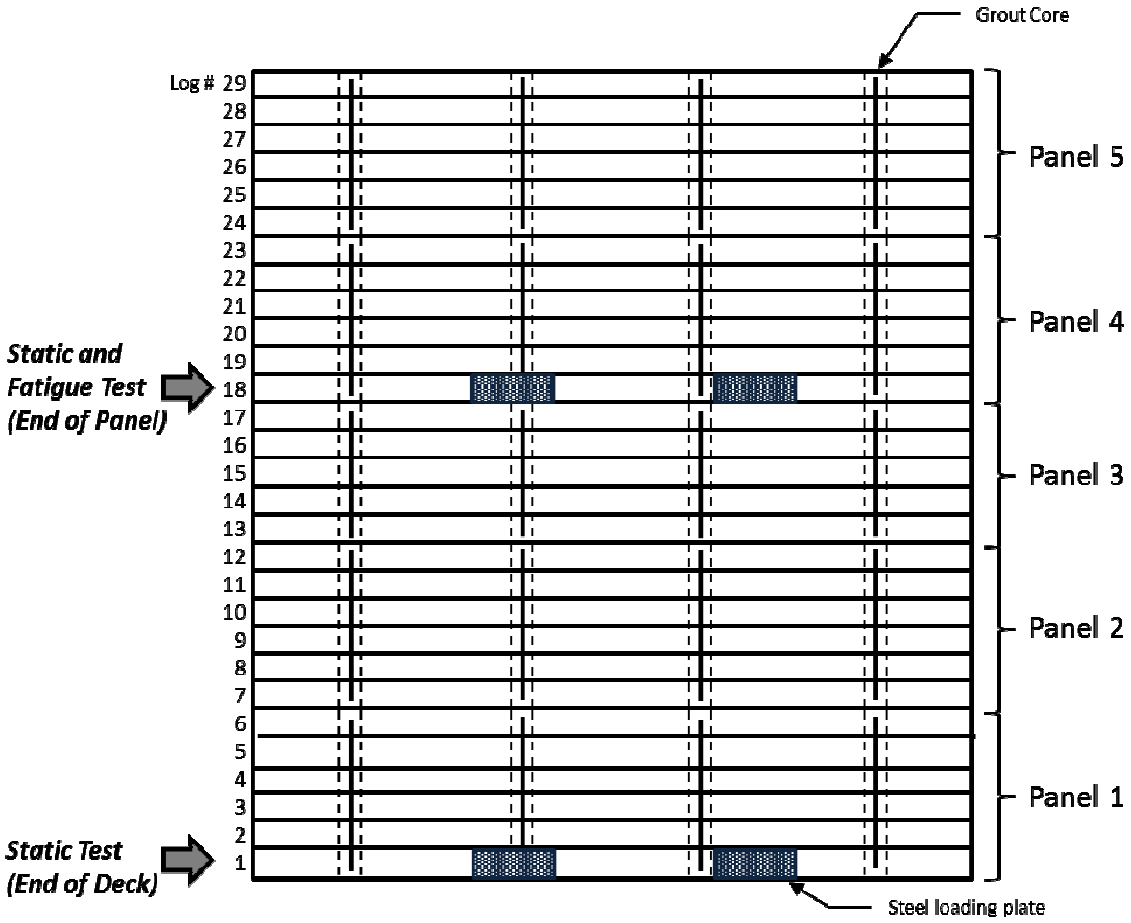

Figure 3-20. Test locations on anchored log deck.

3.5.6 Static Testing

Two static tests were first conducted on the model of the anchored log deck. In the first test, the load was applied directly over the log located at the end of the deck as shown in Figure 3-21. A monotonic load was applied at a rate of 1 mm per minute. This test was a destructive test and loading continued until the load stopped increasing at which point the test was stopped.

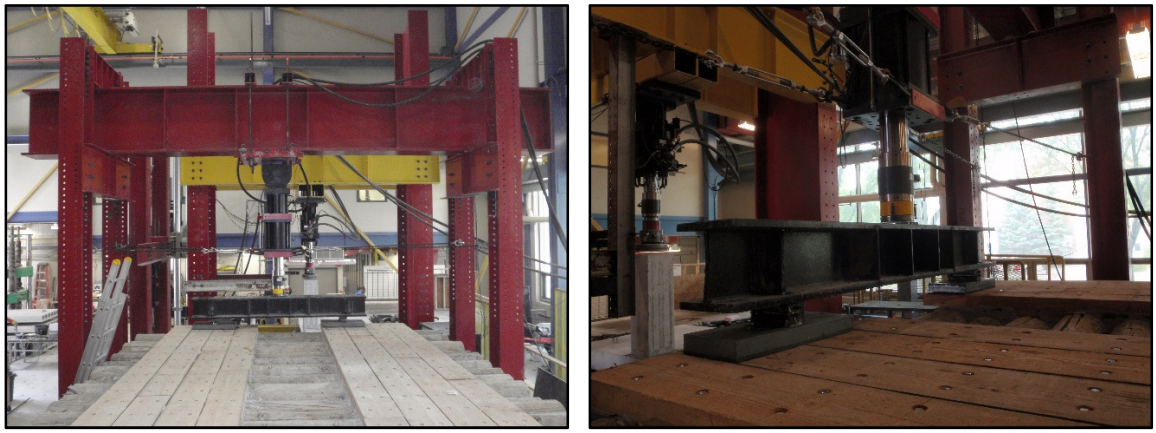

Figure 3-21. First static test location.

The second test was located near the mid-span of the deck. The load was placed over the end log of one panel as shown in Figure 3-22. The purpose of the test was to determine the amount of load distributed to the adjacent panel. A monotonically increasing load was applied until a maximum load of 300 kN was reached and then the load was removed.

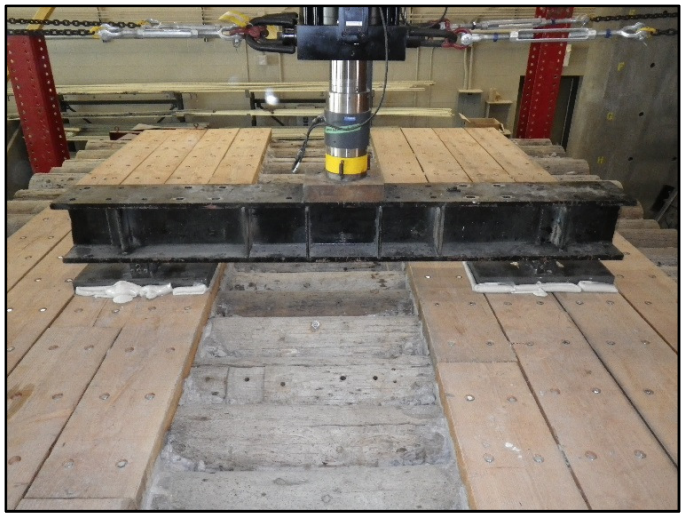

Figure 3-22. Second static test location.

3.5.7 Fatigue Testing

The initial location for the fatigue test was near the opposite end of the deck, approximately between the second and third log from the end (Figure 3-23). Unfortunately, during the setup of the actuator, a large load was applied to the deck accidentally. Before the actuator could be halted, a maximum load of 513 kN had been applied. This resulted in failure of the last two logs at the end of the deck.

Figure 3-23. Initial fatigue test location.

It was decided to move the fatigue test location to the previous second static test location (Figure 3-24). At this location, the load was applied over the end log of a panel. The cyclic (sine wave) loading pattern applied to the deck ranged from a minimum load of 5 kN to a maximum load of 230 kN at a frequency of 0.33 Hz (1 cycle every 3 seconds). In order to maintain a constant loading frequency for the duration of the test, a frequency of 0.33 Hz was chosen. The magnitude of load, 230 kN, chosen for the fatigue test was chosen to be 40% greater than the maximum axle load for a CL-625 truck which is 175 kN (CHBDC 2000). The deck underwent fatigue loading of over 1 million cycles. The results from the fatigue test were used to evaluate the load distribution characteristics between panels under repeated loading.

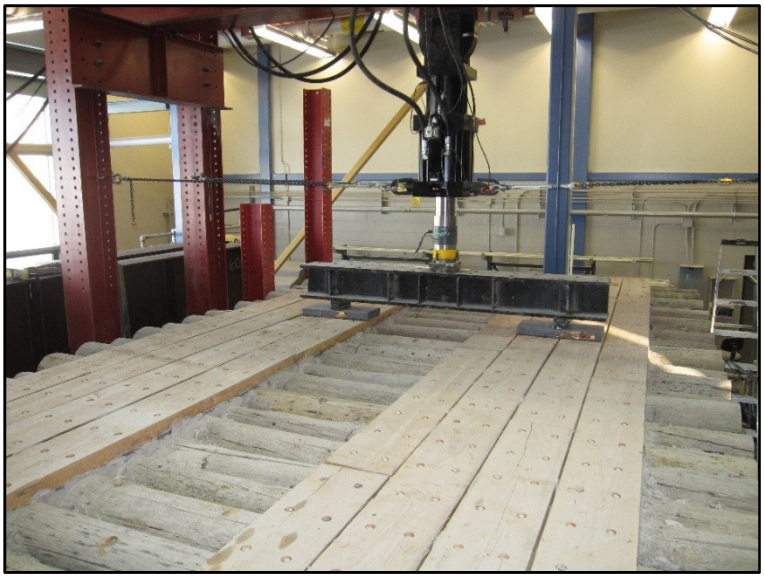

Figure 3-24. Fatigue test location.

After the fatigue loading was completed, a monotonically increasing load was applied at a rate of 2 mm per minute. The loading continued until the load stopped increasing at which point the test was stopped. A final inspection of the deck was performed to assess the damage and take photographs.

4. Experimental Results

4.1 Introduction

During the experimental program, the magnitude of the applied load and displacement of the logs under the test locations were recorded by a National Instruments data acquisition system.

4.2 Log Panel Test Results

4.2.1 Deflection Measurement

The three-log models were instrumented with a linear variable displacement transducer (LVDT) under each log to measure deflection at mid-span (Figures 4-1 a) and b)). Deflections were measured relative to the structural floor. Steel angles were connected to the loading frame and magnetic bases were mounted on the angle to hold the LVDTs in place. Machine screws, glued to the underside of each log, were used to attach to the LVDTs. A LVDT was also placed under each log at one-third span (Figure 4-1).

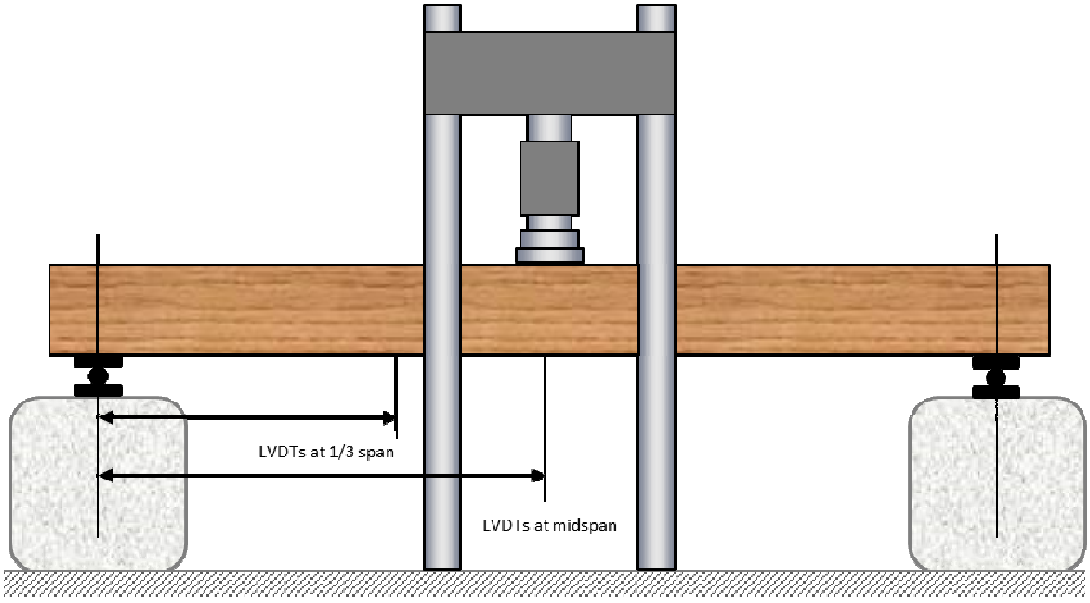

a) Locations of LVDTs during static test of three-log models

b) Placement of LVDTs under each log

Figure 4-1. LVDTs at mid-span and one-third span.

4.2.2 Deflection Profiles

4.2.2.1 Deflected Profiles for Panels with One Grout Core

A total of three panels with one grout core in each were tested under static loading. One panel had planed logs and two panels had round logs. The measured deflections at the mid-span of the panels with the single wheel load on the middle log are shown in Tables 4-1 to 4-3. The EAST and WEST LVDTs show the deflections of the outer logs while the MIDDLE LVDT represents the deflection of the middle log.

Table 4-1. Deflection measurements in planed log panel (Set 2).

Planed Logs Set 2 - 1 Grout Core			
Load (kN)	LVDT EAST (mm)	LVDT MIDDLE (mm)	LVDT WEST (mm)
40	1.5	3.5	2.0
80	3.1	6.7	3.7
120	4.1	9.8	5.1
160	5.4	13.2	6.5
212 (ultimate)	7.7	20.8	6.7

Table 4-2. Deflection measurements from round log panel (Set 1).

Round Logs Set 1 - 1 Grout Core			
Load (kN)	LVDT EAST (mm)	LVDT MIDDLE (mm)	LVDT WEST (mm)
40	0.8	2.3	0.9
80	1.3	5.3	1.5
120	1.4	8.1	1.9
160	1.4	11.4	2.0
214 (ultimate)	0.6	18.8	2.0

Table 4-3. Deflection measurements from round log panel (Set 2).

Round Logs Set 2 - 1 Grout Core			
Load (kN)	LVDT EAST (mm)	LVDT MIDDLE (mm)	LVDT WEST (mm)
40	1.3	3.5	1.0
80	2.0	6.9	0.9
120	2.3	10.5	0.9
160	2.3	12.3	0.6
182 (ultimate)	0.7	23.8	-2.6

4.2.2.2 Deflected Profiles for Panels with Three Grout Cores

A total of five models with three grout cores in each were tested under static loading. Two models had planed logs and three models had round logs, two of which utilized Cintec anchors. The measured deflections at the mid-span for the models with planed and round logs with the single wheel load located at the middle log are shown in Tables 4-4 to 4-8.

Table 4-4. Deflection measurements from planed log panel (Set 1).

Planed Logs Set 1 - 3 Grout Cores			
Load (kN)	LVDT EAST (mm)	LVDT MIDDLE (mm)	LVDT WEST (mm)
40	1.9	3.0	1.8
80	3.6	5.6	3.1
120	5.3	8.1	4.2
160	6.9	10.9	5.3
199 (ultimate)	9.6	15.0	6.5

Table 4-5. Deflection measurements from planed log panel (Set 3).

Planed Logs Set 3 - 3 Grout Cores			
Load (kN)	LVDT EAST (mm)	LVDT MIDDLE (mm)	LVDT WEST (mm)
40	2.0	3.7	2.3
80	3.8	7.0	4.1
120	5.5	10.7	5.6
160	7.3	14.9	7.2
196 (ultimate)	9.2	21.0	8.8

Table 4-6. Deflection measurements from round log panel (Set 3).

Round Logs Set 3 - 3 Grout Cores			
Load (kN)	LVDT EAST (mm)	LVDT MIDDLE (mm)	LVDT WEST (mm)
40	1.6	3.0	1.4
80	3.0	6.4	2.5
120	4.2	10.1	2.8
140	4.7	12.7	2.9
157 (ultimate)	5.1	15.2	2.9

Table 4-7. Deflection measurements from round log with Cintec anchors panel (Set A).

Round Logs with Cintec Anchors Set A - 3 Grout Cores			
Load (kN)	LVDT EAST (mm)	LVDT MIDDLE (mm)	LVDT WEST (mm)
40	1.1	3.6	1.4
80	2.1	7.5	2.4
120	2.8	12.4	3.1
130 (ultimate)	2.9	18.7	3.2

Table 4-8. Deflection measurements from round log with Cintec anchors panel (Set B).

Round Logs with Cintec Anchors Set B - 3 Grout Cores			
Load (kN)	LVDT EAST (mm)	LVDT MIDDLE (mm)	LVDT WEST (mm)
40	1.0	2.9	1.0
80	1.9	5.6	1.5
120	2.5	8.6	1.9
151 (ultimate)	2.9	13.9	1.9

4.2.3 Modes of Failure

When a timber beam is subjected to bending, its one half is subjected to compression parallel to the grain and the other half to tension parallel to the grain. In addition, horizontal shear is induced parallel to the grain. During the tests, the log models failed in a number of ways. A typical failure of a panel with planed logs is shown in Figure 4-2. In this figure, the middle log sustained the largest deformation and failed in tension. A tension failure consists of cracking and splitting in the tension zone where wood is weak in tension perpendicular to the grain. The outer log on the left side failed in horizontal shear along the grain near the neutral axis and the failure around the grout core of the log is shown in Figure 4-3. In the panels with the round logs, the failure mode was predominately in the tension of the middle log (Figure 4-4).

Figure 4-2. Deformation and tension failure in planed log panels.

Figure 4-3. Horizontal shear failure around grout core.

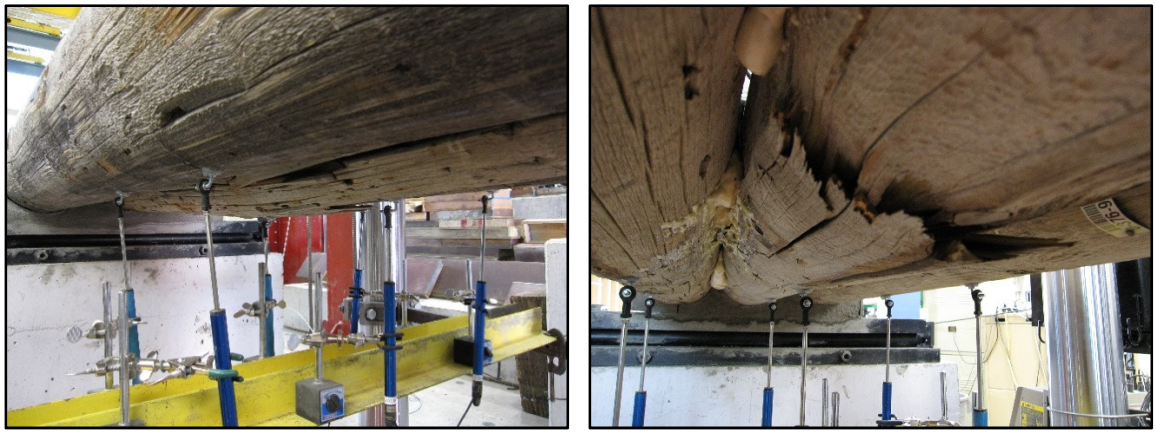

Figure 4-4. Tension failure of round log panels.

4.3 Log Deck Test Results

4.3.1 Deflection Measurement

A total of 13 LVDTs were used to measure displacements of the logs during the static and fatigue tests of the anchored log deck. All LVDTs were connected to a data acquisition system which recorded the readings along with the load and stroke measurements of the actuator.

4.3.2 Static Test (End of Deck)

The first static test was conducted with the load on the log located at the end of the deck (Log #1). The LVDTs were placed in a longitudinal line under the first 13 logs. The line was located under the center of the load plate farthest from the girder, approximately 995 mm from the center of the girder and denoted as Section A-A in Figure 4-5. The LVDTs were numbered according to the log numbers (Figure 4-5).

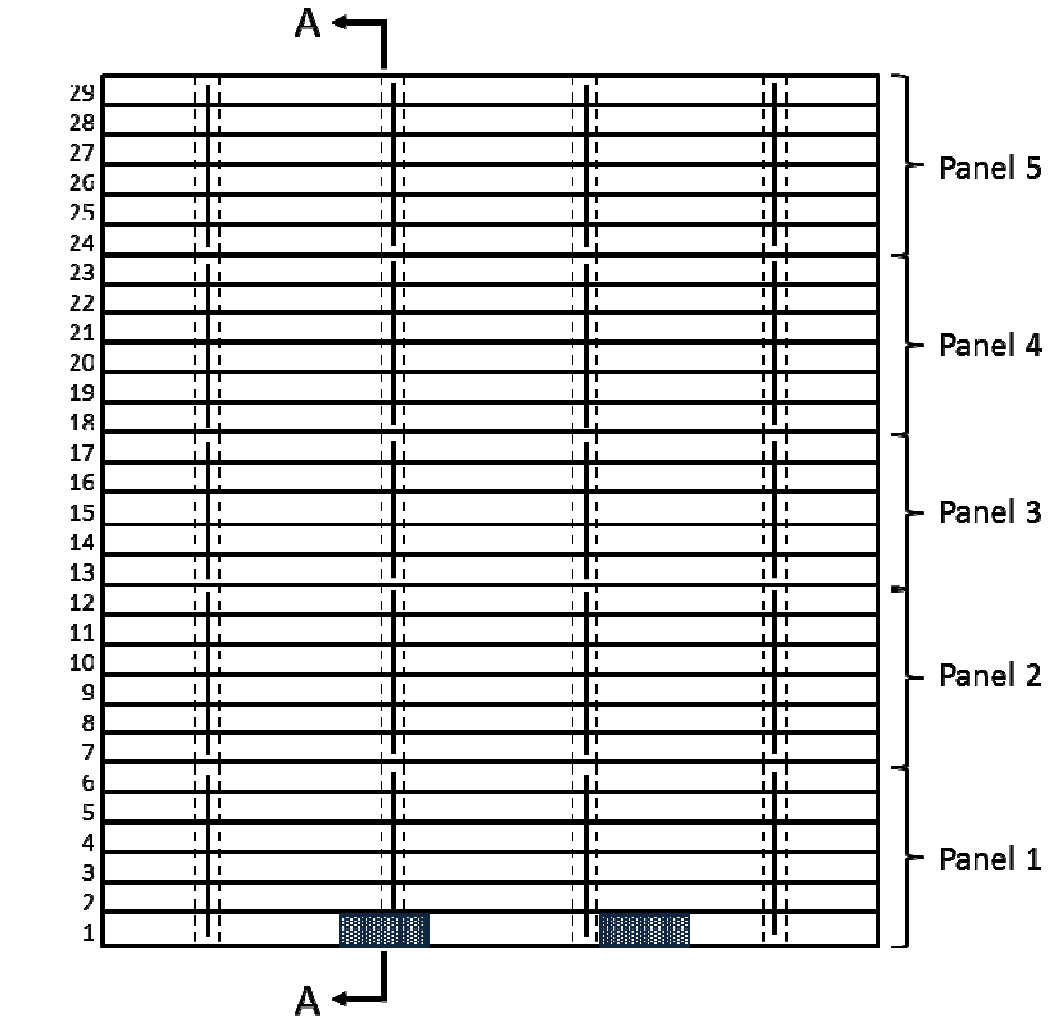

Plan view

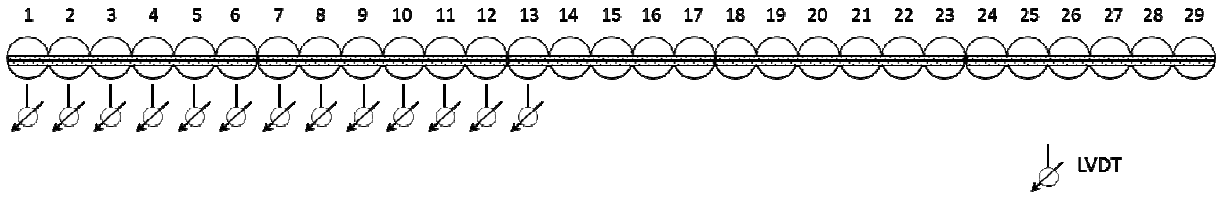

Cross section 'A-A'

Figure 4-5. Location of LVDTs for first static test location.

During the test, the wearing planks under the load plate failed at 432 kN (Figure 4-6). The loading continued to a maximum load of 468 kN. At the ultimate load, the outer log (Log #1) directly under the load exhibited a tension and horizontal shear failure as shown in Figure 4-7. The load-deflection plots corresponding to the static test are presented in Figure 4-8. The behavior of the logs is fairly linear until the load reaches approximately 325 kN. After this level of load, the logs start to behave non-linearly as the deck begins to show signs of failure.

Figure 4-6. Failure of wearing plank.

Figure 4-7. Tension and horizontal shear failure of outer log.

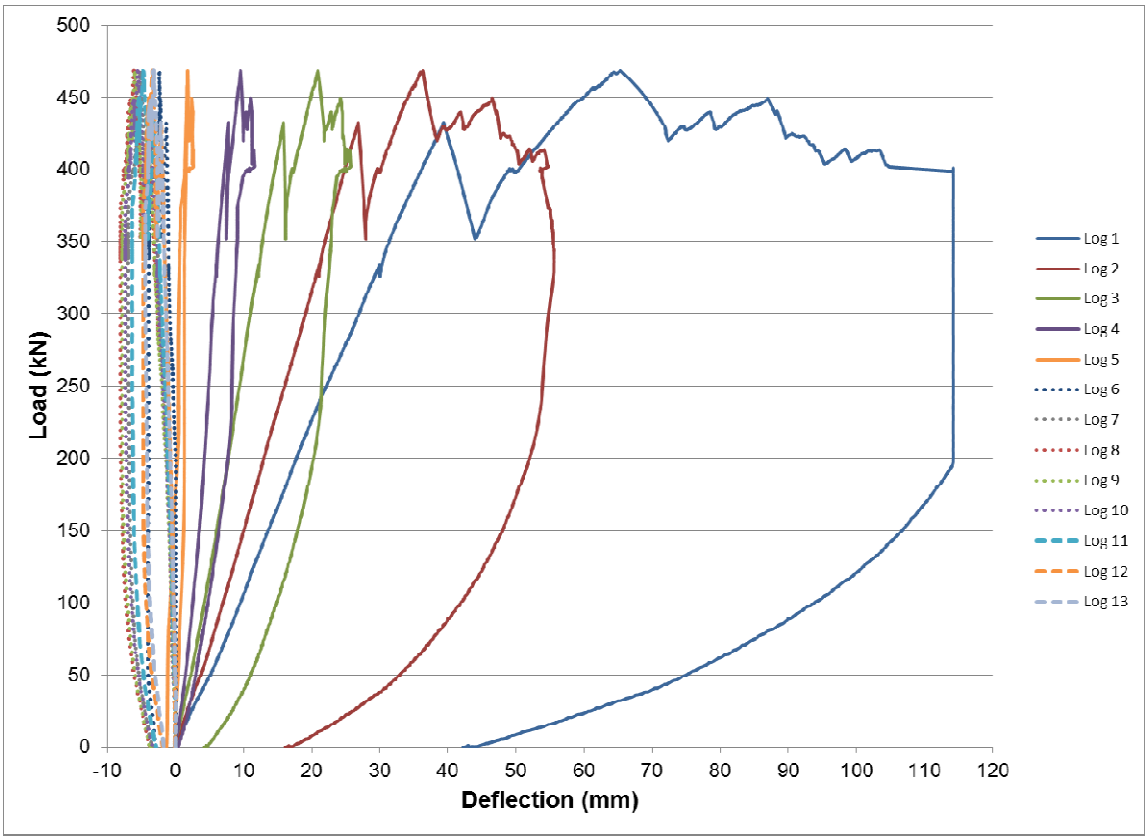

Figure 4-8. Load vs deflection for static test (end of deck).

The deflections of the logs under the static test at 100 kN, 200 kN, 300 kN and the ultimate load of 468 kN are listed in Table 4-9. It is noted that Logs #6 to 13 exhibit negative deflection which indicates the logs uplifted during the test. This is a result of the application of load at the end of the deck over Log #1.

Table 4-9. Log deflections (mm) for first static test location.

Load (kN)	Log No.												
	1	2	3	4	5	6	7	8	9	10	11	12	13
100	9.53	6.99	4.24	2.56	0.78	0.08	-0.35	-0.56	-0.55	-0.50	-0.35	-0.15	-0.21
200	17.79	12.99	7.78	4.26	1.33	0.05	-1.00	-1.32	-1.38	-1.26	-1.05	-0.66	-0.76
300	26.90	19.06	11.02	5.48	1.34	-0.77	-2.22	-2.61	-2.69	-2.39	-1.98	-1.30	-1.41
468 (ultimate)	65.36	36.36	20.93	9.56	1.79	-2.31	-5.15	-6.12	-5.96	-5.57	-4.76	-3.40	-3.22

4.3.3 Static Test (End of Panel)

For the second static test, the load was placed over the end log of one panel near the mid-span. The load was applied over Log #18. LVDTs were placed under Logs #12 to 24 as shown in Section A-A in Figure 4-9. A monotonically increasing load was applied until a load of 300 kN was reached at which point the loading was removed.

The deflections of the logs under the static test at 100 kN, 200 kN, and 300 kN are listed in Table 4-10.

Table 4-10. Log deflections (mm) for second static test location

Load (kN)	Log No.												
	12	**13**	**14**	**15**	**16**	**17**	**18**	**19**	**20**	**21**	**22**	**23**	**24**
100	0.33	0.71	1.35	2.46	3.28	4.84	5.59	6.06	5.17	3.81	2.87	1.96	1.25
200	0.05	0.84	2.16	3.97	5.67	8.78	10.29	10.66	8.86	6.65	4.85	3.40	2.02
300	-0.02	1.13	2.97	5.53	8.17	12.47	14.72	14.87	12.11	9.10	6.46	4.55	2.62

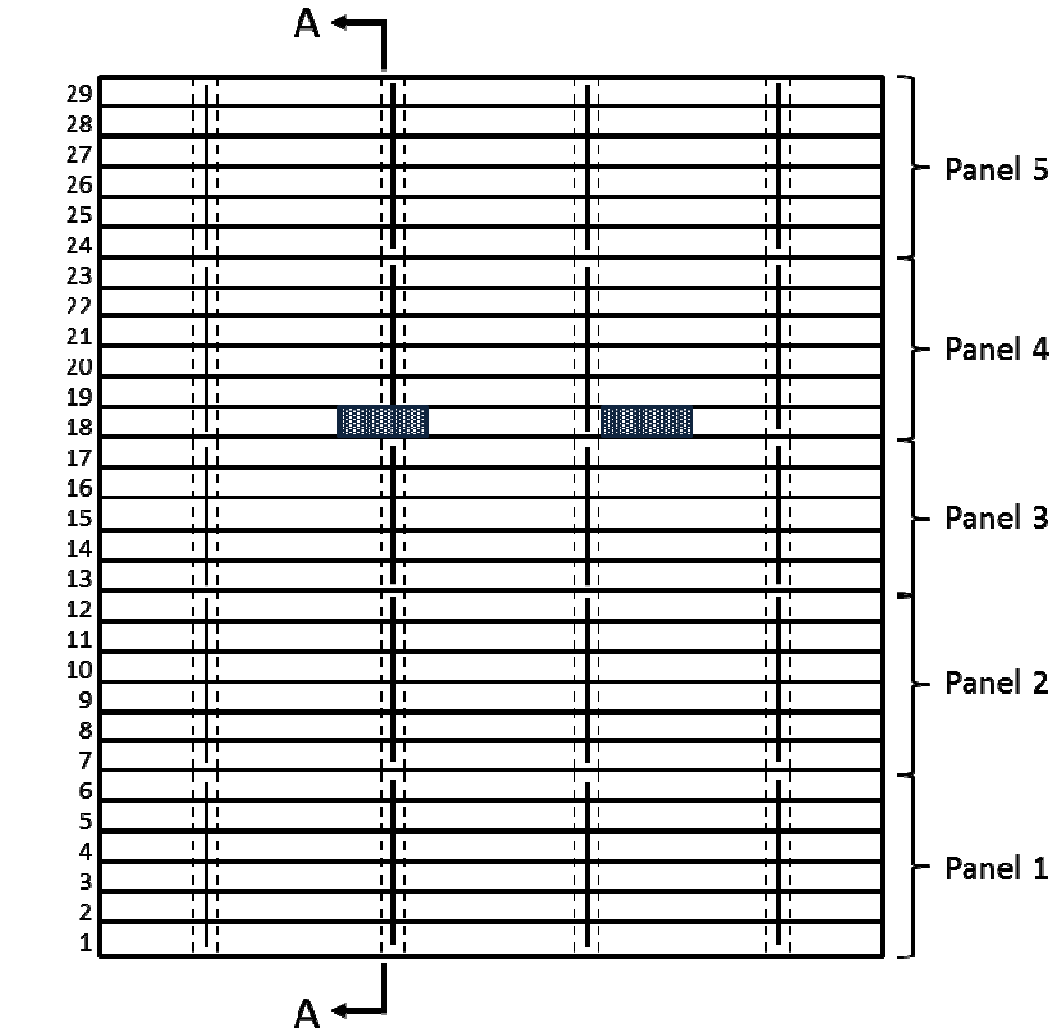

Plan view

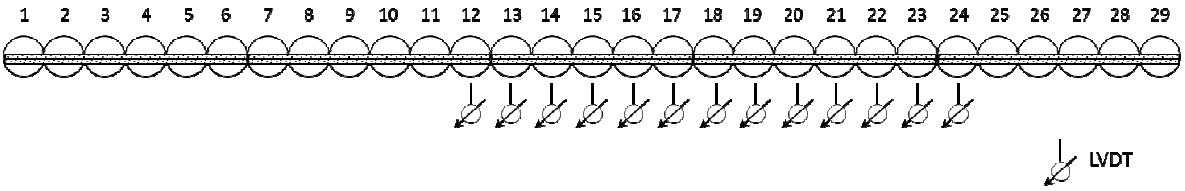

Cross section 'A-A'

Figure 4-9. Location of LVDTs for second static test location.

4.3.4 Fatigue and Static Test (End of Panel)

Due to the accidental over-loading and failure of the logs at the initial fatigue test location near the end of the deck, the fatigue test was conducted at the second static test location. The load was applied over Log #18 which is the end log of one panel near the mid-span. The instrumentation scheme was similar to that of the second static test (Figure 4-9) except that Log #12 was not instrumented. The locations of LVDTs are shown in Figure 4-10.

A cyclic load ranging from 5 to 230 kN was applied at a rate of one cycle every 3 seconds (0.33 Hz). Over 1 million cycles was applied to the deck under this fatigue loading rate. Plots of the deflection of Log #18 over the course of the fatigue loading are shown in Figure 4-11. In this figure, the deflections can be seen to be increasing steadily with the number of applied cycles.

Figure 4-10. LVDTs located underneath the deck.

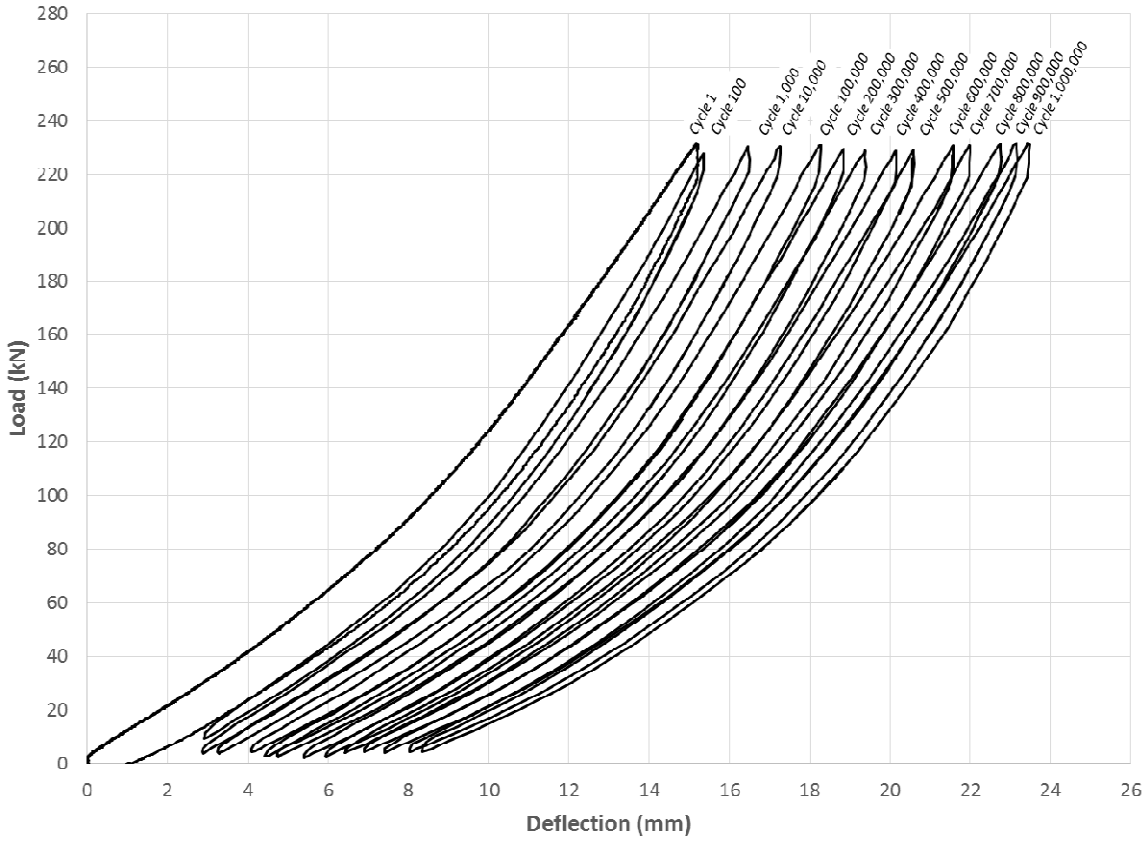

Figure 4-11. Load vs deflection of Log #18 under fatigue testing (end of panel).

Over the course of the fatigue test, the deflection of Log #18 increased from 15.12 mm to 23.42 mm as shown in Figure 4-12. During the first 10,000 cycles, the deflection increased approximately 2.17 mm to 17.29 mm. At this point the rate of deflection decreased and for the following cycles, the deflection steadily increased an additional 6.13 mm.

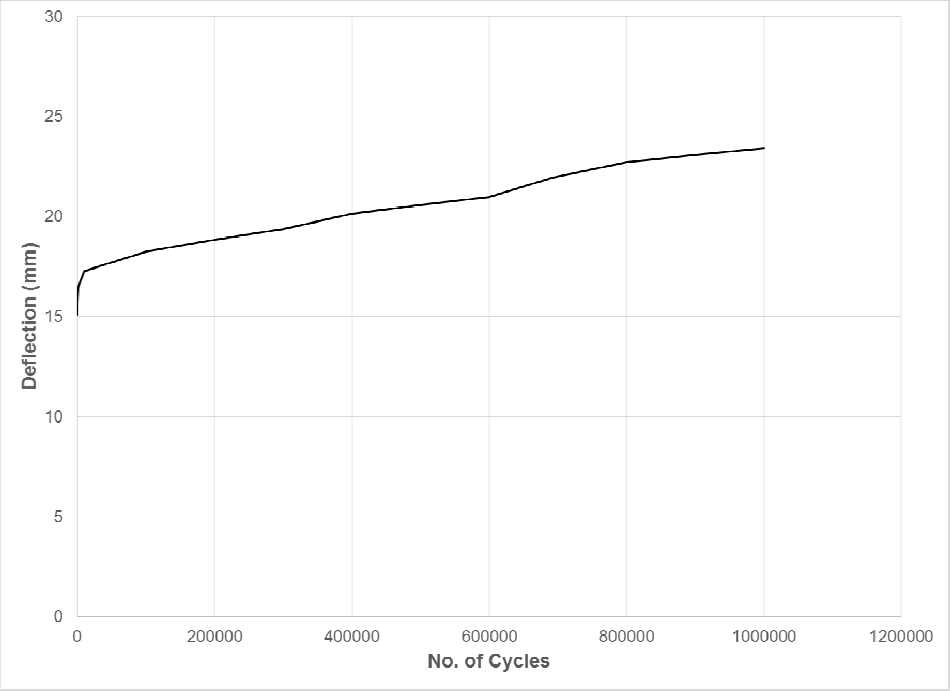

Figure 4-12. Deflection vs number of cycles of Log #18 during fatigue loading.

The deflections of the instrumented logs at 230 kN at specific cycles are summarized in Table 4-11. The table shows the gradual increase in deflection of the adjacent logs. However, the logs farthest from the load show very little change in deflection over the course of the fatigue loading. This indicates the majority of the load transfer occurs only between several logs on either side of the load location.

Table 4-11. Log deflections (mm) at 230 kN during fatigue test

Cycle	Log No.											
	13	**14**	**15**	**16**	**17**	**18**	**19**	**20**	**21**	**22**	**23**	**24**
1	1.63	3.35	6.15	9.45	13.57	15.12	13.69	11.36	8.57	6.29	4.58	2.98
10,000	2.06	3.92	7.30	11.29	15.84	17.29	15.68	12.96	10.31	7.03	5.56	3.44
100,000	2.03	3.92	7.53	12.16	16.93	18.24	16.91	13.95	10.90	7.50	5.85	3.49
500,000	1.87	4.01	7.82	12.10	19.12	20.58	19.17	16.21	11.41	8.16	5.83	3.67
1,000,000	2.17	4.70	8.20	13.8	22.04	23.42	22.23	18.76	13.40	9.40	6.17	3.58

After the fatigue loading was completed, a static load test was conducted at the same location. A monotonically increasing load was applied to a maximum of 614 kN at which point the load suddenly dropped. The stroke of the actuator continued to increase, but the load did not reach the ultimate load. The loading was stopped and removed when it became clear that the deck was not receiving additional load. Upon inspection after the test, it was observed that Log #17 exhibited a horizontal shear failure as shown in Figure 4-13. Inspection of the underside of the logs revealed large splits in Logs #17 and 19 (Figure 4-14). However, no obvious signs of tension failure were found.

A plot of the load and deflection of the instrumented logs is shown in Figure 4-15. All the logs behaved linearly until reaching a load of approximately 100 kN where the slopes became steeper. The log deflections continued increasing linearly at this slope until the load reached 320 kN where the logs started to behave in a non-linear manner. In Figure 4-15, as the load increases, there are small drops in the load due to the development of splits and cracks in the logs which contribute to the failure at the ultimate load.

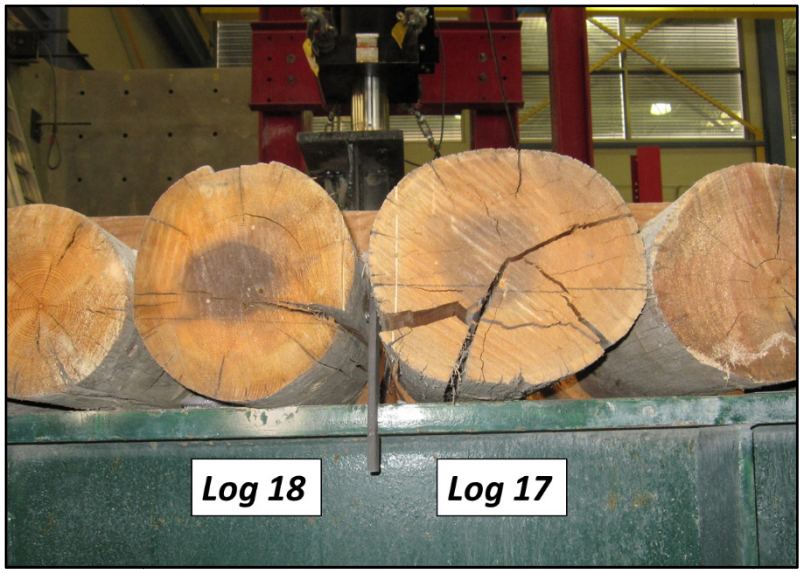

Figure 4-13. Horizontal shear failure of Log #17.

Figure 4-14. View of underside of logs after static test.

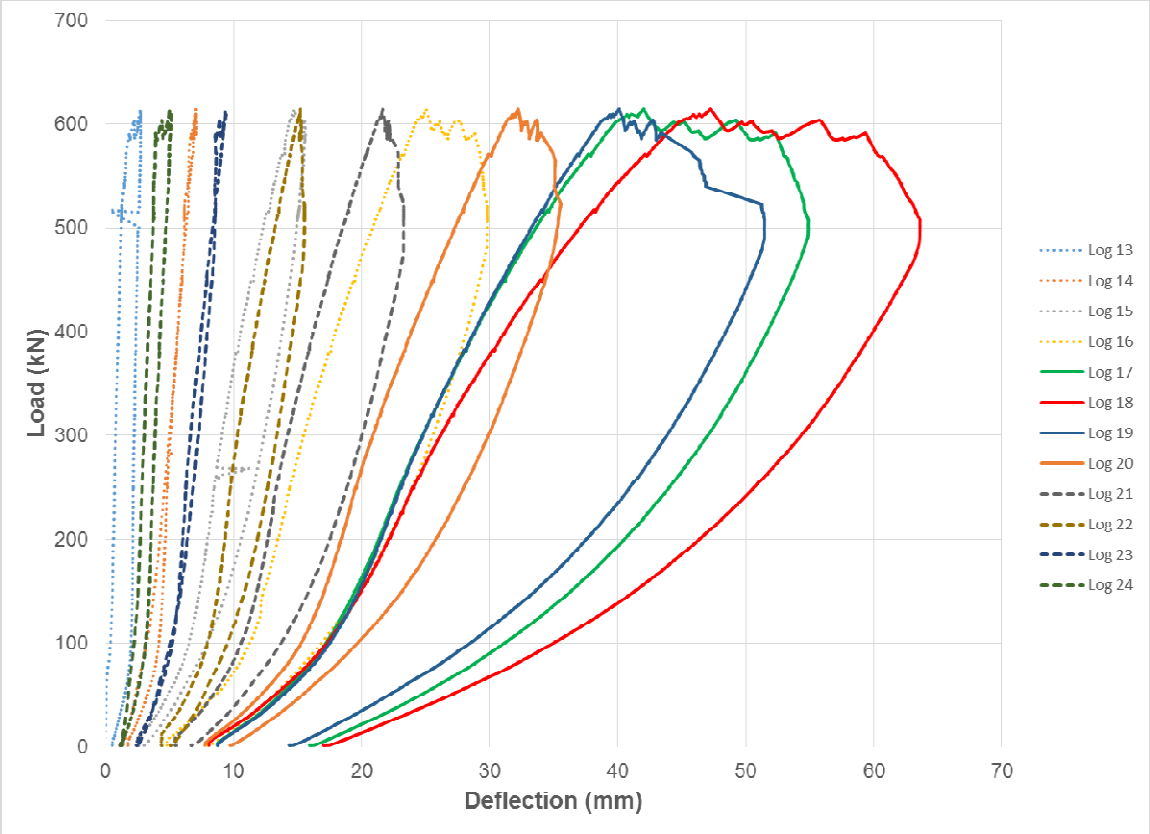

Figure 4-15. Load vs deflection for static test (end of panel).

5. Discussion and Analytical Model

5.1 Introduction

This chapter discusses the load distribution behavior of the three-log models and the full bridge deck model based on the results from the static and fatigue tests. An analytical model of the anchored log bridge deck is also presented.

5.2 Log Panel Tests

A total of eight three-log models were tested under static loading applied to the middle log; three of the models were constructed with planed logs and the remaining five with round logs. All the panels initially had one grout core at the mid-span. However, after testing three panels (one planed and two round log), it was observed the grout core only at the mid-span was not efficient in transferring loads between logs. Thus, additional grout cores were added at the quarter and three quarter span length to the remaining five panels.

From the static tests, it was observed the three-log models with the planed logs displayed better load distribution characteristics than the models with round logs. This is likely due to friction between the planed faces of the logs. At a load of 120 kN, the deflections of the outer logs (denoted as East and West) and the middle log (denoted as Mid) are shown in Figure 5-1. In the figure, the difference in deflections between the outer and middle logs for the planed log panels is much less than in the round log panels. However, a decision was made to conduct further research on with round logs, because the high cost of trimming the logs was very high. One reason for the high cost is the lack of contractors

willing to perform the work. The contractors were hesitant to work with treated logs as extra precautions would have to be taken to contain the preservative-laden sawdust. Also, due to the possibility of embedded nails in the logs, the contractors did not want to risk damage to their equipment.

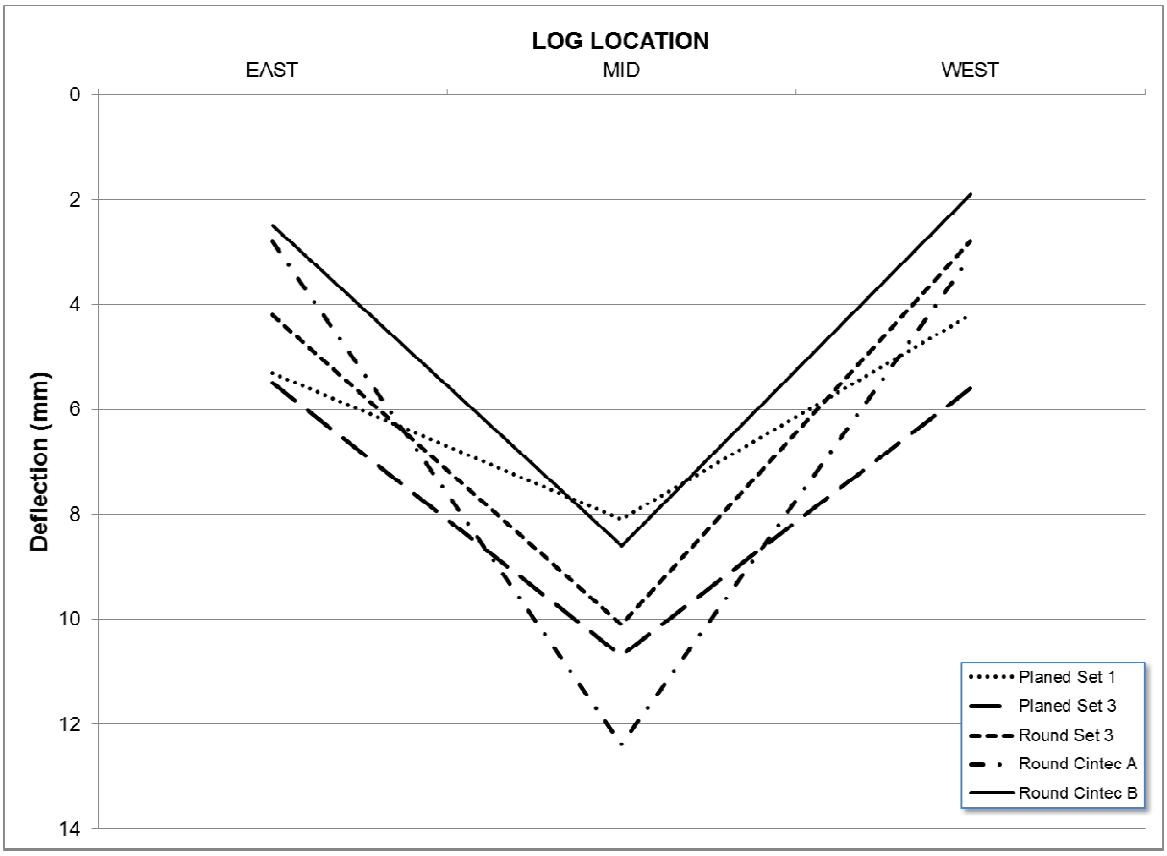

Figure 5-1. Deflection of logs at 120 kN for panels with three grout cores.

5.3 Log Deck Tests

Three static tests and one fatigue test were conducted on the full-scale model of the anchored log deck. The deck was constructed with five log panels incorporating a total of 29 logs. The panels were connected to each other with lag screws and wearing planks were installed on top of the logs. High density foam was injected between the planks and logs to fill the remaining gaps between them. The load was applied through two steel

plates which simulated the footprint of the dual tire of a heavy truck. The steel plates were located eccentrically on the deck, where one plate was placed at the edge of the wearing plank.

5.3.1 Static Test (End of Deck)

The first static test was conducted with the concentrated load placed over the log located at the end of the deck. A monotonically increasing load was applied until failure. The log deflections at the ultimate load of 468 kN are shown in Figure 5-2.

Figure 5-2. Deflection measurements across the logs at 468 kN.

The first panel consisted of Logs #1 to 6, the adjacent panel included Logs #7 to 12 and Log #13 was the end log of the third panel. In Figure 5.2, the first five logs deflected

under the load distribution. Logs #6 to 13 experienced a negative deflection indicating that the second and third panels lifted up slightly from the girders as a result of the applied load at the end of the deck. At the ultimate load, the largest upward deflection was 6.1 mm which is small compared to the 72.0 mm deflection the loaded Log #1.

5.3.2 Static Test (End of Panel)

A static test was conducted with the concentrated load over the end log, #18, of a panel located near the mid-span. The load was increased to a maximum of 300 kN after which the loading was removed. The purpose of the test was to determine the load distribution characteristics of the deck. The deflections at the maximum load of 300 kN are shown in Figure 5-3. The load was applied over Log #18.

Figure 5.3. Deflection measurements across the logs at 300 kN.

5.3.2.1 Distribution factor

The distribution factor for deflections, as defined by Limaye (1999), is the ratio of the deflection of a log and the average deflections of all the logs. This factor provides a method to compare the performance of the log panels. A high value of the distribution factor for the loaded log indicates poor load distribution characteristics. The equation for the distribution factor for a log is:

$$DF = \frac{\delta}{\delta_{avg}} \quad [5.1]$$

where δ is the deflection of a log at a given transverse section, and δ_{avg} is the average deflection of all the logs at the same transverse section. The distribution factors for the instrumented logs in the second static test are listed in Table 5-1. As a check, it is confirmed that the average distribution factor is 1. Based on the values in the table, the majority of the load is distributed to the logs closest to the applied load location.

Table 5-1. Distribution factors of instrumented logs in second static test.

	Log No.												
	12	**13**	**14**	**15**	**16**	**17**	**18**	**19**	**20**	**21**	**22**	**23**	**24**
DF	0.00	0.16	0.41	0.76	1.12	1.71	2.02	2.04	1.66	1.25	0.89	0.62	0.36

5.3.3 Fatigue Test (End of Panel)

A fatigue test was conducted with the load at the same location as in the second static test, i.e over Log #18. The deck was subjected to over 1 million cycles of load; this number is considered adequate as the deck is proposed for low-volume bridges. The deflections of the instrumented logs over the course of the fatigue loading tests at the maximum load of 230 kN are shown in Figure 5-4. One deck panel consisted of Logs #13

to 17 and the adjacent panel comprised of Logs #18 to 23. Log #24 represents the end of the next adjacent panel. As expected, the maximum deflection was under Log #18. The load distribution pattern across the logs does not change significantly as the number of loading cycles increase; however, the magnitude of deflections does increase with the number of cycles.

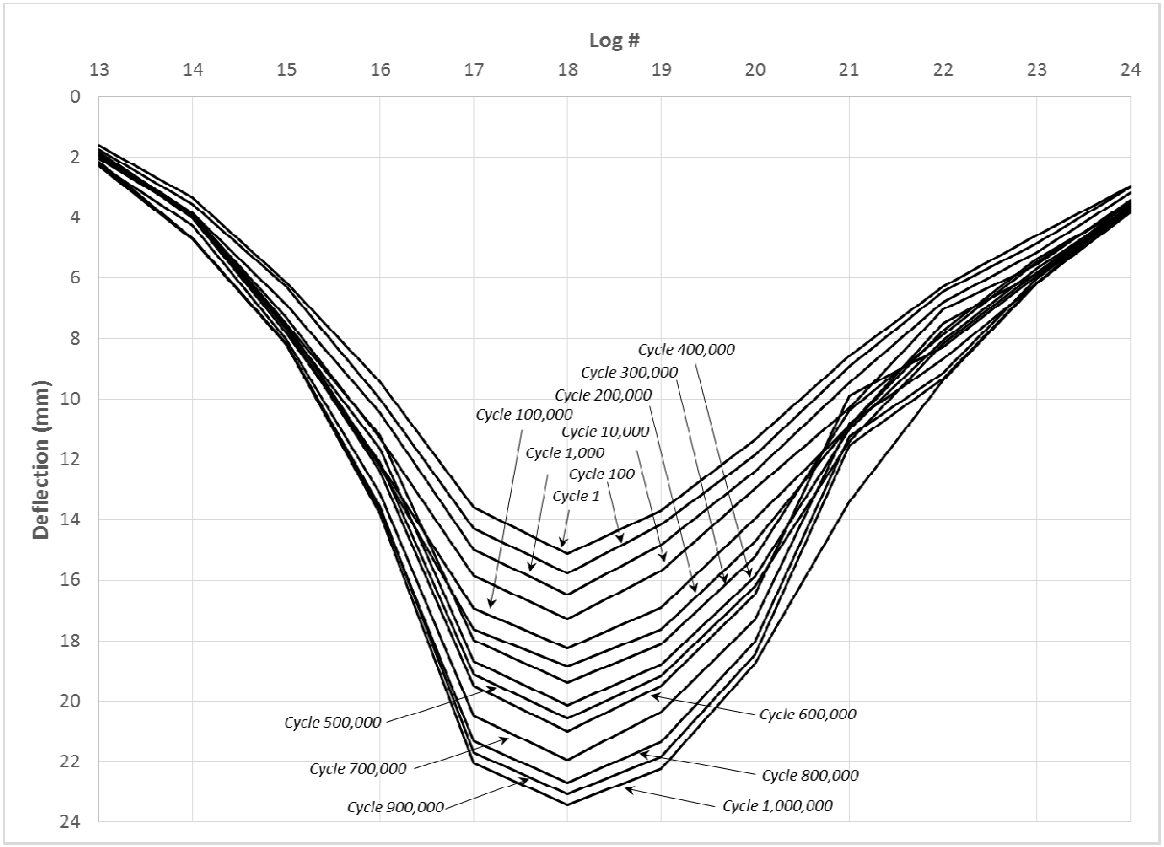

Figure 5-4. Deflections of logs at 230 kN during fatigue loading.

The progression of the distribution factor for the deck over the course of the fatigue loading is shown in Table 5-2. In the table, the distribution factor only slightly increases as the number of cycles increase.

Table 5-2. Progression of distribution factor for Log #18 during fatigue test.

Cycle #	Log #18 Deflection (mm)	DF
1	15.12	1.88
100	15.77	1.88
1,000	16.47	1.86
10,000	17.29	1.84
100,000	18.24	1.83
200,000	18.85	1.85
300,000	19.37	1.90
400,000	20.14	1.90
500,000	20.58	1.90
600,000	20.98	1.94
700,000	21.95	1.92
800,000	22.70	1.91
900,000	23.07	1.91
1,000,000	23.42	1.90

5.3.4 Static Test after Fatigue Cyclic Loading (End of Panel)

After the deck was subjected to fatigue loading of over 1 million cycles, a static test was conducted with the load at the same location. A monotonically increasing load was applied over Log #18 until failure. The deflections of the instrumented logs at various load levels are shown in Figure 5-5. The maximum load reached during the tests was 614 kN just prior to a sudden drop in load. Based on the deflections in Figure 5-5, at lower loads, there is a larger distribution of load across adjacent logs. However, as the load increases, the distribution pattern tends become localized so that a large portion of the load is taken by three logs, Logs #17 to 19. The pattern of transverse distribution of loads becomes more and more localized as the load is increased. Although the load is

transferred to the end log (Log #17) of the adjacent panel, the remaining logs in the panel (Logs #13 to 16) receive smaller magnitudes of load.

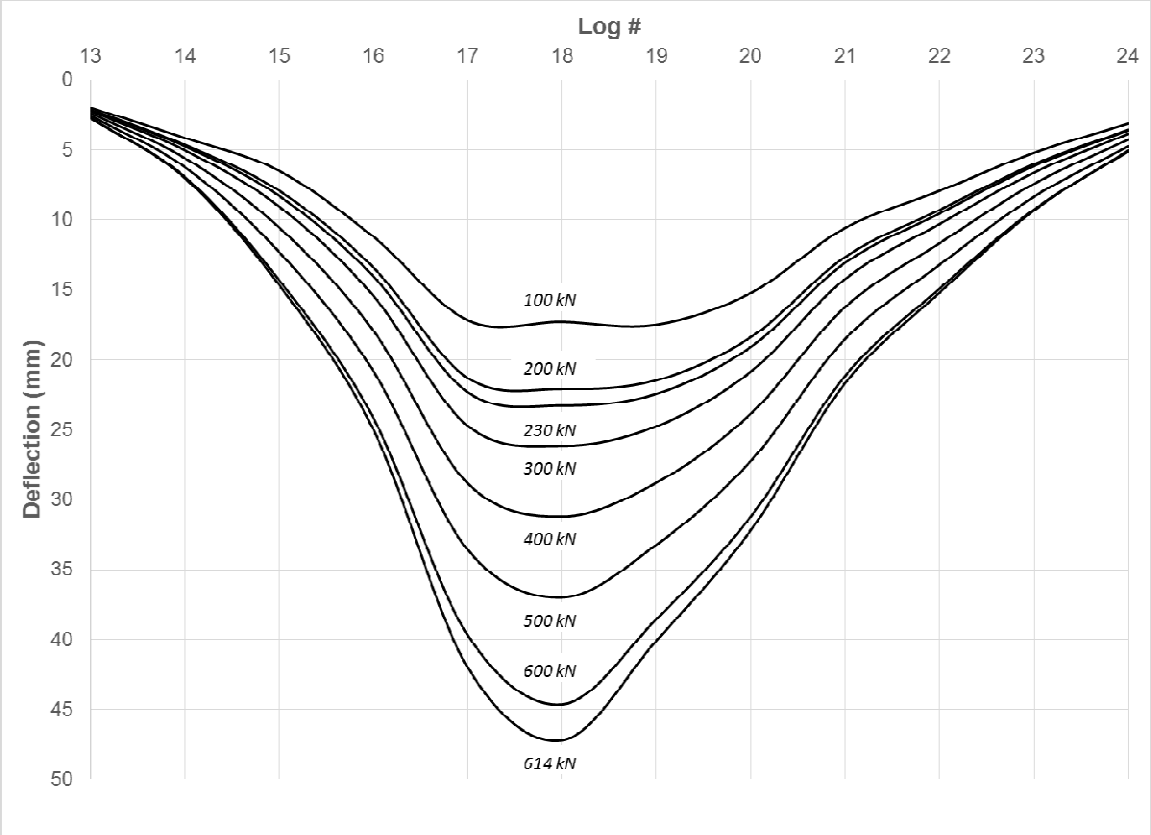

Figure 5-5. Deflections of logs during static test.

5.4 Analytical Model

The analysis of log decks is a complex process due to the orthotropic nature of both the wood and their assembly as decks. The mechanical properties of wood are different along each axis. One method that can be used for the idealization of a slab-on-girder bridge for live load analysis is the semi-continuum method (Jaeger and Bakht 1985). This method was developed as an alternative to the grillage and orthotropic plate methods. In the semi-continuum idealization, the bridge structure is modelled as discrete longitudinal members

with a continuous transverse medium; it is an accurate method to determine the load distribution between the girders.

A software program called SECAN was developed (Mufti et al., 2003) to implement the semi-continuum method for analysis of bridges. The program calculates the bending moment, shear and deflection at any user defined section.

The anchored log deck was analyzed using the SECAN program and the loading scheme was based on the second static test. In this case, the deck was modelled as 13 longitudinal beams with a continuous transverse medium. Each beam represented a log and the medium represented the wearing planks. The input parameters for the SECAN program include the span length, elastic and shear modulus of the girder and slab, moment of inertia, torsional moment of inertia and load locations. The user can input the reference location(s) where the program will perform its analysis.

The elastic modulus used for the SECAN program was based on the stiffness tests conducted for the logs in the three log models. Using the data from the stiffness tests, the elastic modulus in the longitudinal direction (E_L) was calculated for each log and the average E_L was 8070 MPa. The relationship between the elastic modulus and shear modulus for a timber log is:

$$G_L = 0.061E_L \qquad [5.2]$$

Where G_L is the shear modulus in the longitudinal direction. In this case, G_L = 492 MPa.

Since the size of the logs varied, the moment of inertia and torsional moment of inertia was calculated for each log. The moment of inertia was determined using the following expression:

$$I = \frac{\pi d^4}{64} \quad [5.3]$$

Where d is the diameter of the log. The torsional moment of inertia was calculated using:

$$J = \frac{\pi d^4}{32} \quad [5.4]$$

The values for I and J are found in Table 5-3.

Table 5-3. Moments of inertia and torsional moments of inertia of instrumented logs.

	Log No.												
	12	**13**	**14**	**15**	**16**	**17**	**18**	**19**	**20**	**21**	**22**	**23**	**24**
I ($mm^4 x10^8$)	2.04	2.51	2.38	2.16	2.66	2.33	1.63	1.26	1.47	1.50	1.15	2.29	2.47
J ($mm^4 x10^8$)	4.07	5.03	4.75	4.32	5.31	4.66	3.26	2.52	2.93	3.00	2.30	4.47	4.93

The oak wearing planks represented the slab material in the SECAN analysis. The E of the slab was assumed to be 11,000 MPa and the corresponding value for G was 671 MPa. The reference location was set at the same location as the longitudinal line of LVDTs and the parameters were used for the input file of the program. The program was executed for a load of 300 kN. The thickness of the slab in the program was adjusted until the resulting load distribution pattern matched that obtained experimentally from the second static test. Various values for thickness were tested and the results for slab thicknesses of 45 mm, 64 mm and 85 mm are summarized in Table 5-4. The actual thickness of the wearing planks was 64 mm. As the slab thickness increases to 85 mm, the values for deflection for Logs #17 to 24 become closer to the experimental values. However, the difference

increases for Logs #12 to 16. Conversely, as the thickness decreases to 45 mm, the deflection values for Logs #12 to 16 approach the experimental results while Logs #17 to 24, with the exception of Log #20, increase in difference. This demonstrates that the distribution of load is not the same in two panels. The load is successfully transferred to the end log (#17) of the adjacent panel. However, a smaller proportion than predicted by SECAN is transferred to the remaining logs of the same panel. Another observation is SECAN cannot predict the uplift behavior of Log #12 which was also noted by Klowak (2001). The experimental results and the results from SECAN are compared graphically in Figure 5-6.

Table 5-4. Comparison of experimental and analytical values for deflection of log deck.

Deflection (mm)	Log No.												
	12	**13**	**14**	**15**	**16**	**17**	**18**	**19**	**20**	**21**	**22**	**23**	**24**
Experim.	-0.02	1.13	2.97	5.53	8.17	12.47	14.72	14.87	12.11	9.10	6.46	4.55	2.62
SECAN (45mm)	0.45	1.31	2.82	5.51	9.69	15.16	20.51	16.90	11.87	7.27	3.89	1.77	0.59
% difference	3069	15.1	5.22	0.36	18.6	21.5	39.4	13.7	2.0	20.1	39.8	61.1	77.3
SECAN (64mm)	0.35	1.83	3.78	6.48	9.90	13.56	17.17	14.75	11.68	8.26	5.21	2.78	0.93
% difference	2367	61.2	27.4	17.2	21.2	8.7	16.7	0.79	3.58	9.27	19.4	38.8	64.3
SECAN (85 mm)	0.68	2.51	4.59	7.00	9.65	12.13	14.85	12.95	11.01	8.55	6.05	3.75	1.71
% difference	4587	121	54.6	26.7	18.0	2.76	0.91	12.9	9.11	6.07	6.34	17.5	34.9

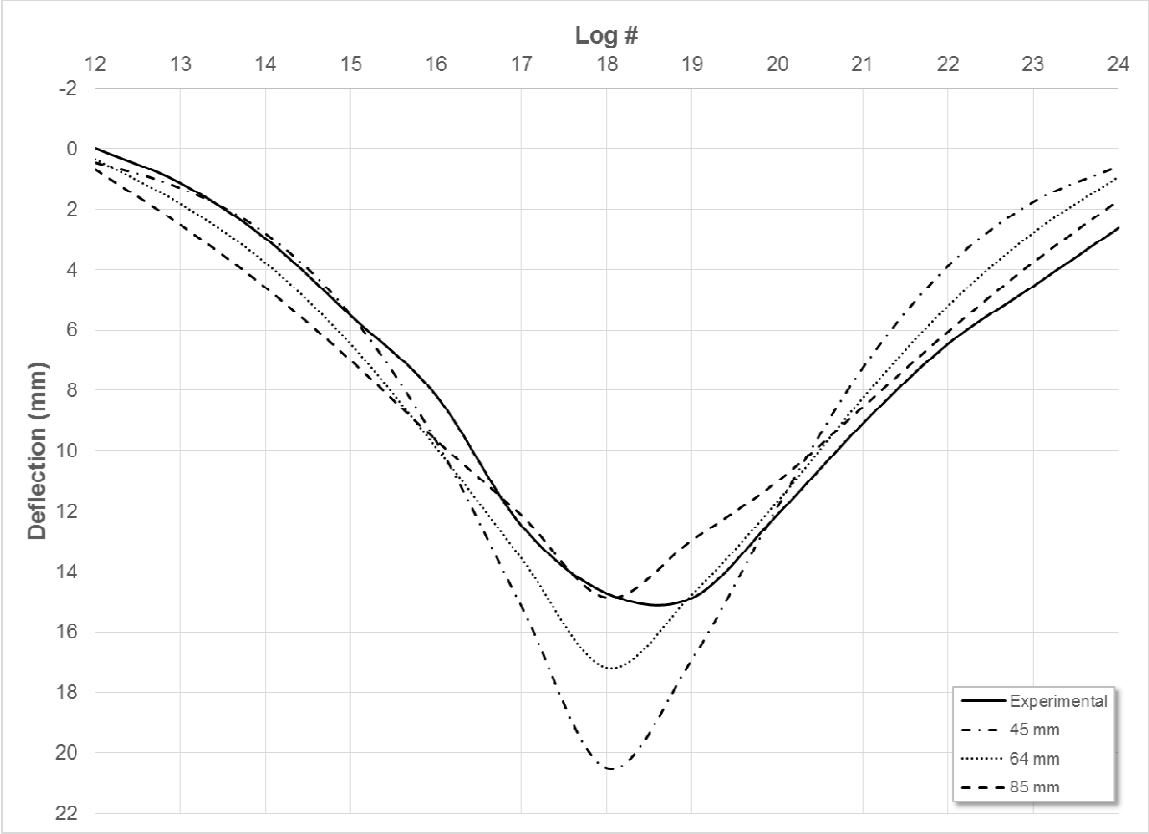

Figure 5-6. Comparison of experimental and SECAN results.

6. Conclusions and Recommendations

6.1 Summary

This research program investigated the construction and performance of the anchored log deck. The anchored log deck is the next generation of wood bridge decks and is intended mainly for use on the winter roads of Manitoba and on short span bridges. While the research program considered bridges only for low-volume roads, there is no reason to believe that the anchored log deck should be limited to this application.

Previous research on grout laminated decks found that the grout lamination technique is effective in transverse load distribution. The anchored log deck constructed in this research consisted of multiple panels with round logs, with unstressed reinforced grout cores placed at four locations along the log panels. Lag screws connected the panels together and timber planks were installed on top of the panels as the wearing course. High-density expanding foam was placed in between the logs and planks to fill the gaps. Static and fatigue testing was conducted at different locations on the deck to test its load sharing characteristics. A software program, SECAN, was used to model the deck using the semi-continuum method. The analytical and experimental results were then compared.

The following conclusions can be drawn from this research program:

[1] The anchored log deck system with unstressed reinforced grout cores, wearing planks and expanding foam exhibits adequate load distribution characteristics.

[2] Lag screws and wearing planks play a significant role in the load transfer between logs.

[3] The load sharing between adjacent panels is not symmetric when the load is located at the end of one panel.

[4] Discarded utility poles have the potential to be recycled into anchored log decks. Since the utility poles have a preservative treatment, they do not require additional protection from the environment for durability.

[5] Grout lamination of round logs using Cintec anchoring technology is an effective method to prevent the leakage of grout in the grout cores. Another advantage is their ease of installation.

[6] Modular design of log deck panels allow flexibility to accommodate different bridge span lengths.

6.2 Recommendations

The following recommendations can be made based on the conclusions above:

[1] Further research on the load distribution characteristics of the anchored log deck including additional test locations.

[2] Further consideration on simplifying the construction method for the anchored log deck as well as developing a process for its disassembly.

[3] Research additional alternatives for connecting adjacent panels which can improve the load sharing characteristics.

[4] Further research on fatigue life of anchored log deck.

[5] Design and testing of a confining system for the end logs of the deck.

REFERENCES

Bakht, B., Jaeger, L.G., and Klubal, J. (1994). Observed prestress losses in stress-laminated wood decks. *Proceedings of the 4th International Conference on Short and Medium Span Bridges*, Halifax, N.S., 8–11 August 1994. Edited by A.A. Mufti, B. Bakht, and L.G. Jaeger. Canadian Society for Civil Engineering, Montréal, Que. pp. 743–753.

Bakht, B., Lam, C., and Bolshakova, T. (1997). The first stressed log bridge. *Proceedings of US-Canada-Europe Workshop on Bridge Engineering,* Zurich, Switzerland pp. 155–162.

Bakht, B., Maheu, J., and Bolshakova, T. (1996). Stressed log bridges. *Canadian Journal of Civil Engineering,* 23(2): 490–501.

CHBDC (2000). Canadian Highway Bridge Design Code, *Canadian Standards Association International*. Toronto, Ontario, Canada.

Concrete Restoration Services (2013). CRS 486 U-LIFT Foam Technology System, http://www.concrete-restoration.mb.ca/CRS.html

Csagoly, P.F. and Taylor, R.J. 1980. A structural wood system for highway bridges. IABSE Proceedings International Association for Bridge and Structural Engineering: 35-80. Zurich, Switzerland.

Jaeger, L.G. and Bakht, B. (1985). Bridge analysis by the semi-continuum method. *Canadian Journal of Civil Engineering,* Vol. 12(3):573-582.

Klowak, C. (2001). The Flexural Behaviour of Grout Laminated Log Decks, *Project Report submitted to Department of Civil Engineering, Faculty of Engineering, University of Manitoba,* Winnipeg, Canada.

Kuryk, D. (2003). Winter Roads in Manitoba. *Proceedings on the 12th Workshop on the Hydraulics of Ice Covered Rivers,* Edmonton, AB, June 19-20, 2003.

Limaye, V. (1999). Experimental and Analytical Investigation on Grout Laminated Log Decks, *Master of Applied Science Thesis submitted to Faculty of Engineering, Dalhousie University,* Halifax, Nova Scotia, Canada.

Mufti, A.A., Bakht, B., Jaeger, L.G. and Jalali, J. (2003). SECAN4 User Manual – Incorporating the Semi-Continuum Method of Analysis for Bridges, *ISIS Canada Research Network Technical Report,* Winnipeg, Manitoba, Canada.

Ritter, M.A., 1990, Timber Bridges: Design, Construction, Inspection and Maintenance. *United States Department of Agriculture,* August 1992. Washington, DC, USA.